

## II. REMARKS

### Formal Matters

Claims 1, 2, 4, 7-9, 11, 12, 16-18, and 20-28 are pending after entry of the amendments set forth herein.

Claims 1-14 and 16-28 were examined and were rejected. Claim 15 was withdrawn from consideration.

Claims 1, 4, 8, 11, 18, and 24 are amended. The amendments to the claims were made solely in the interest of expediting prosecution, and are not to be construed as acquiescence to any objection or rejection of any claim. No new matter is added by these amendments.

Claims 3, 5, 6, 10, 13-15, and 19 are canceled without prejudice to renewal, without intent to acquiesce to any rejection, and without intent to surrender any subject matter encompassed by the canceled claims. Applicants expressly reserve the right to pursue any canceled subject matter in one or more continuation and/or divisional applications.

Applicants respectfully request reconsideration of the application in view of the remarks made herein.

### Withdrawn rejections

Applicants note with gratitude that the following rejections, made in the August 10, 2005 Office Action, were withdrawn: 1) rejection of claims 1, 3-8, and 10-14 under 35 U.S.C. §102(b); and 2) rejection of claims 2 and 9 under 35 U.S.C. §103(a).

### Rejections under 35 U.S.C. §112, first paragraph

Claims 5, 6, 14, 20, and 25 were rejected under 35 U.S.C. §112, first paragraph, as allegedly lacking written description. Claims 1-14 and 16-28 were rejected under 35 U.S.C. §112, first paragraph, as allegedly lacking enablement. Claims 1-14 and 16-28 were rejected under 35 U.S.C. §112, first paragraph, as allegedly lacking written description.

Written description: claims 5, 6, 14, 20, and 25

Claims 5, 6, 14, 20, and 25 are canceled without prejudice to renewal, thereby rendering any rejection of these claims moot.

The Office Action stated that support for “Arc mRNA” and “ERK mRNA” could not be found. Applicants note that paragraph 0021 states that a “calcium-responsive gene product” refers to a protein and/or an mRNA whose level varies with the intracellular calcium concentration. Paragraph 0021 states that calcium-responsive gene products include a phospho-extracellular signal-regulated kinase (phospho-ERK or p-ERK) gene product. Paragraph 0052 states that other examples of calcium-responsive gene products are immediate early gene products such as c-Fos and Arc.

Enablement: claims 1-14 and 16-28

The Office Action stated that the specification does not reasonably provide enablement for a method of detecting an amyloid peptide-related neurological disorder, or a method of identifying a candidate agent for treating an amyloid peptide-related neurological disorder, comprising detecting a level of any calcium-responsive gene product in the brain of any non-human animal model.

*Amyloid peptide-related neurological disorders*

Impairment of spatial learning is but one amyloid peptide-related neurological disorder that can be detected using a claimed method. As discussed in the instant application, the claimed methods provide for detection of amyloid peptide-related neurological disorders including impaired spatial learning, impaired memory, and behavioral deficits.

As discussed in Palop et al. ((2003) *Proc. Natl. Acad. Sci. USA* 100:9572-9577; “Palop 2003”; a copy of which is provided herewith as Exhibit 1), altered levels of calcium-responsive gene products such as calbindin and c-Fos reflect various Alzheimer’s Disease (AD)-related cognitive impairments and behavioral deficits.

*Calcium-responsive gene products*

Applicants’ position on this issue has been made of record. As discussed previously, the specification provides *working examples* of **four** calcium-responsive gene products whose levels are altered in an animal model of an amyloid peptide-related neurological disorder. The four calcium-responsive gene products for which working examples are presented are **c-fos, calbindin, neuropeptide**

**Y**, and  **$\alpha$ -actinin-II**. A person skilled in the art would find it reasonable that the levels of other calcium-responsive gene products are affected in amyloid peptide-related neurological disorders.

Furthermore, Palop et al. ((2005) *J. Neurosci.* 25:9686-9693; “Palop 2005”; a copy of which is provided herewith as Exhibit 2) provides further evidence for the fact that altered levels of the calcium-responsive gene product Arc correlate with amyloid peptide-related neurological disorders. Palop 2005 shows that the expression of hAPP/A $\beta$  decreases the expression of Arc, both at baseline and after environmental stimulation, particularly in the granule cells of the dentate gyrus. Still further, Chin et al. ((2005) *J. Neurosci.* 25:9694-9703; “Chin”; a copy of which is provided herewith as Exhibit 3) provides further evidence for the fact that altered levels of the calcium-responsive gene product phospho-ERK correlate with amyloid peptide-related neurological disorders. Chin provides evidence that the tyrosine kinase Fyn can cooperate with A $\beta$  in the depletion of calcium-responsive proteins.

Thus, in addition to the **four working examples** of calcium-responsive gene products, levels of the Arc and phospho-ERK gene products, which are discussed in the patent application, have been shown to be correlated with an amyloid peptide-related neurological disorder. Thus, **at least six** calcium-responsive gene products are disclosed in the instant specification; and altered levels of all six of these calcium-responsive gene products have been shown to be correlated with amyloid peptide-related neurological disorders. In addition, as described in Chin 2005, levels of the calcium-responsive gene Fyn have been shown to be correlated with an amyloid peptide-related neurological disorder.

#### *Non-human animal model*

Applicants' position on this issue has been made of record. As discussed previously, the instant specification provides numerous references describing animal models of amyloid peptide-related neurological disorders such as AD. There is no requirement that the animal model of the amyloid peptide-related neurological disorder comprise a transgene encoding a mutant APP. The specification provides sufficient enablement such that one of ordinary skill in the art would be able to practice the invention without undue experimentation. Accordingly, the instant claims meet the enablement requirement of 35 U.S.C. § 112, first paragraph.

Written description; claims 1-14 and 16-28

The Office Action stated that the rejection of claims 1-14 and 16-28 as lacking written description was made for reasons of record in the Office Action mailed August 10, 2005. The August 10, 2005 Office Action stated that the specification “teaches only the gene products of CB, c-Fos, neuropeptide Y, and  $\alpha$ -actinin II are affected in level in response to expression of amyloid peptide.” August 10, 2005 Office Action, page 13.

As noted above, in addition to the **four working examples** of calcium-responsive gene products, levels of two additional calcium-responsive gene products, namely Arc and phospho-ERK gene products, which are discussed in the patent application, have been shown to be correlated with an amyloid peptide-related neurological disorder. Thus, at least six calcium-responsive gene products are described in the patent application, where altered levels are correlated to an amyloid peptide-related neurological disorder.

Conclusion as to the rejections under 35 U.S.C. §112, first paragraph

Applicants submit that the rejections of the claims discussed above under 35 U.S.C. §112, first paragraph, have been adequately addressed in view of the remarks set forth above. The Examiner is thus respectfully requested to withdraw the rejections.

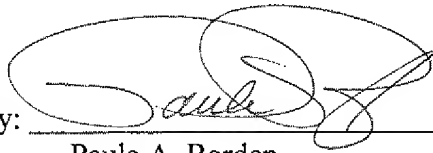
### III. CONCLUSION

Applicants submit that all of the claims are in condition for allowance, which action is requested. If the Examiner finds that a telephone conference would expedite the prosecution of this application, the Examiner is invited to telephone the undersigned at the number provided.

The Commissioner is hereby authorized to charge any underpayment of fees associated with this communication, including any necessary fees for extensions of time, or credit any overpayment to Deposit Account No. 50-0815, order number UCAL-280.

Respectfully submitted,  
BOZICEVIC, FIELD & FRANCIS LLP

Date: Oct. 26, 2006

By:   
Paula A. Borden  
Registration No. 42,344

BOZICEVIC, FIELD & FRANCIS LLP  
1900 University Avenue, Suite 200  
East Palo Alto, CA 94303  
Telephone: (650) 327-3400  
Facsimile: (650) 327-3231

# Neuronal depletion of calcium-dependent proteins in the dentate gyrus is tightly linked to Alzheimer's disease-related cognitive deficits

Jorge J. Palop\*, Brian Jones\*, Lisa Kekoni\*, Jeannie Chin\*, Gui-Qiu Yu\*, Jacob Raber\*†, Eliezer Masliah‡, and Lennart Mucke\*§

\*Gladstone Institute of Neurological Disease and Department of Neurology, University of California, San Francisco, CA 94141; and ‡Departments of Neurosciences and Pathology, University of California at San Diego, La Jolla, CA 92093

Communicated by Robert W. Mahley, The J. David Gladstone Institutes, San Francisco, CA, June 3, 2003 (received for review March 20, 2003)

Transgenic mice expressing human amyloid precursor proteins (hAPP) and amyloid- $\beta$  peptides ( $A\beta$ ) in neurons develop phenotypic alterations resembling Alzheimer's disease (AD). The mechanisms underlying cognitive deficits in AD and hAPP mice are largely unknown. We have identified two molecular alterations that accurately reflect AD-related cognitive impairments. Learning deficits in mice expressing familial AD-mutant hAPP correlated strongly with decreased levels of the calcium-binding protein calbindin-D<sub>28k</sub> (CB) and the calcium-dependent immediate early gene product c-Fos in granule cells of the dentate gyrus, a brain region critically involved in learning and memory. These molecular alterations were age-dependent and correlated with the relative abundance of  $A\beta$ 1–42 but not with the amount of  $A\beta$  deposited in amyloid plaques. CB reductions in the dentate gyrus primarily reflected a decrease in neuronal CB levels rather than a loss of CB-producing neurons. CB levels were also markedly reduced in granule cells of humans with AD, even though these neurons are relatively resistant to AD-related cell death. Thus, neuronal populations resisting cell death in AD and hAPP mice can still be drastically altered at the molecular level. The tight link between  $A\beta$ -induced cognitive deficits and neuronal depletion of CB and c-Fos suggests an involvement of calcium-dependent pathways in AD-related cognitive decline and could facilitate the preclinical evaluation of novel AD treatments.

The bright prospect of increasing life expectancy in many populations around the world is tempered by an alarming increase in aging-related neurodegenerative disorders (1). Alzheimer's disease (AD), the most frequent of these conditions, causes inexorable loss of memory and other cognitive functions. Although the etiology of most AD cases remains elusive, the analysis of related transgenic (TG) mouse models is beginning to unravel the pathogenic importance of specific AD-associated molecules (2–8). These models are also used increasingly to assess novel AD treatments (9–13). Amyloid plaques are the primary pathological outcome measure in these studies, although their contribution to AD-related cognitive deficits is uncertain (4–6, 8, 14–16). Indeed, there is an urgent need to pinpoint reliable surrogate markers of  $A\beta$ -induced cognitive decline and to unravel the pathways that disrupt neuronal functions in AD and related conditions.

We studied TG mice in which neuronal expression of human amyloid precursor proteins (hAPP) is directed by the platelet-derived growth factor  $\beta$  chain promoter (6). Mice from line J20 express familial AD-mutant (K670N, M671L, V717F; hAPP770 numbering) hAPP (hAPP<sub>FAD</sub>) and have high levels of human amyloid- $\beta$  peptides ( $A\beta$ ) in the hippocampus (6), which is heavily affected in AD and critically involved in learning and memory (17–19). We analyzed the expression of calcium-dependent proteins in the hippocampus and their relationships with cognitive deficits in hAPP<sub>FAD</sub> mice and AD, because neuronal calcium homeostasis and calcium signaling likely play

critical roles in learning and memory as well as in the pathogenesis of AD (20–23).

## Materials and Methods

**TG Mice and Behavioral Testing.** Line J20 produces hAPP with the Swedish and Indiana FAD mutations; line I5 produces WT hAPP (hAPP<sub>WT</sub>) at comparable levels (6, 24). Mice represent F<sub>6</sub>–F<sub>10</sub> offspring of heterozygous TG mice and C57BL/6J non-TG breeders.

Unless indicated otherwise, measurements were performed on gender-balanced groups. Male mice were tested in a Morris water maze essentially as described (14); see *Supporting Text*, which is published as supporting information on the PNAS web site, [www.pnas.org](http://www.pnas.org), for details. Anesthetized mice were flushed transcardially with PBS. One hemisphere was fixed in 4% phosphate-buffered paraformaldehyde at 4°C for 48 h, and the other was stored at –70°C. All experiments were approved by the committee on animal research of the University of California, San Francisco.

**Human Tissues.** Fixed brain tissues of AD cases [nine women, six men; age 71–92 yr (83.7 ± 6.7, mean ± SD)] and nondemented controls (one woman, one man; age 71 and 74 yr) were from the Alzheimer's Disease Research Center (University of California at San Diego). AD was determined according to criteria of the Consortium to Establish a Registry for Alzheimer's Disease and the National Institute on Aging. Formalin-fixed hippocampal tissues were postfixed for 72 h in 4% phosphate-buffered paraformaldehyde.

**Immunohistochemistry.** Vibratome sections (50  $\mu$ m, mouse; 40  $\mu$ m, human) or sliding microtome sections (30  $\mu$ m, mouse) were used for fluorescence double-labeling or staining with standard avidin-biotin/oxidase methods. After quenching endogenous peroxidase activity and blocking nonspecific binding, sections were incubated first with rabbit anticalbindin (1:15,000, Swant, Bellinzona, Switzerland); rabbit anti-c-Fos (1:10,000, Ab-5, Oncogene); mouse mAb anti-Neu-N (1:5,000, Chemicon); or mouse mAb anti- $A\beta$  (1:500, 3D6, Elan Pharmaceuticals, South San Francisco, CA), and then with fluorescein-labeled donkey anti-rabbit (1:300, Jackson ImmunoResearch); Texas red-labeled donkey anti-mouse (1:300, Jackson ImmunoResearch); biotinylated goat anti-rabbit (1:200, Vector Laboratories); or biotinylated goat anti-mouse (1:600, Vector Laboratories). Diaminobenzidine was used as a chromogen. Immunofluorescence was visualized by confocal microscopy.

Abbreviations:  $A\beta$ , amyloid- $\beta$  peptides; AD, Alzheimer's disease; CB, calbindin-D<sub>28k</sub>; hAPP, human amyloid precursor proteins; hAPP<sub>FAD</sub>, familial AD-mutant hAPP; hAPP<sub>WT</sub>, WT hAPP; IR, immunoreactivity/immunoreactive; TG, transgenic.

†Present address: Departments of Behavioral Neuroscience and Neurology, Oregon Health and Science University, Portland, OR 97239.

§To whom correspondence should be addressed. E-mail: [lmucke@gladstone.ucsf.edu](mailto:lmucke@gladstone.ucsf.edu).

**Quantitation of Immunoreactive Structures.** Digitized images were obtained with a DEI-470 digital camera (Optronics, Goleta, CA) on a BX-60 microscope (Olympus, Melville, NY). For calbindin-D<sub>28k</sub> (CB) immunoreactivity (IR), two coronal sections (300  $\mu$ m apart) per mouse between -2.54 and -2.80 mm from bregma were selected. Integrated optical density (IOD) was determined with BioQuant Image Analysis (R&M Biometrics, Nashville, TN) and averaged in two areas (0.04 mm<sup>2</sup> each) of the molecular layer of the dentate gyrus and of the stratum radiatum of the CA1 region. Relative CB-IR levels were expressed as the ratio of IODs in the molecular layer and in the stratum radiatum of the same section. The mean ratio of non-TG mice was defined as 1.0. Relative numbers of c-Fos-IR granule cells were determined by counting c-Fos-IR cells in the granular layer in every 10th serial coronal section throughout the rostrocaudal extent of the granular layer. The average percentage area of the hippocampus occupied by A $\beta$ -IR deposits was determined in four coronal sections (300  $\mu$ m apart) per mouse.

**Western Blot and Quantitative Fluorogenic RT-PCR.** Hemibrains were sectioned with a vibratome into 450- $\mu$ m sagittal slices, and the dentate gyrus was microdissected on ice. For protein analysis, dentate gyrus samples were individually sonicated at 4°C in buffer containing 10 mM Hepes at pH 7.4, 150 mM NaCl, 50 mM NaF, 1 mM EDTA, 1 mM DTT, 1 mM PMSF, 1 mM Na<sub>3</sub>VO<sub>4</sub>, 10  $\mu$ g/ml leupeptin, 10  $\mu$ g/ml aprotinin, and 1% SDS and centrifuged at 5,000  $\times$  g (10 min). Equal amounts of protein (by Bradford assay) were resolved by SDS/PAGE and transferred to nitrocellulose membranes. After blocking, membranes were labeled with rabbit anti-CB (1:20,000, Swant); mouse mAb anti-hAPP (1:1,000, 8E5, Elan Pharmaceuticals); or mouse mAb anti- $\alpha$ -tubulin (1:100,000, B512, Sigma), and incubated with horseradish peroxidase-conjugated goat anti-rabbit IgG (1:5,000, Chemicon) or goat anti-mouse IgG (1:10,000, Chemicon). Bands were visualized by enhanced chemiluminescence and quantitated by densitometry and QUANTITY ONE 4.0 software (Bio-Rad).

For quantitative fluorogenic RT-PCR, RT reactions contained 120 ng of total RNA (DNase-treated) and random hexamer plus oligo d(T) primers. Diluted reactions were analyzed with SYBR green PCR reagents and an ABI Prism 7700 sequence detector (Applied Biosystems). cDNA levels of CB, hAPP, and GAPDH were determined relative to standard curves from pooled samples. The slope of standard curves, control reactions without RT, and dissociation curves of products indicated adequate PCR quality. Primers: CB, 5'-GGA-AAGGAGCTGCAGAACTTGAT-3', 5'-TTCCGGTGATAG-CTCCAATCC-3'; hAPP, 5'-GAGGAGGATGACTCGGATG-TCT-3', 5'-AGCCACTTCTTCTCCTCTGCTA-3'; GAPDH, 5'-GGGAAGCCCATCACCATCTT-3', 5'-GCCTTCTCCAT-GGTGGTGAA-3'.

## Results

**CB Levels Are Reduced in the Dentate Gyrus of hAPP<sub>FAD</sub> Mice and Humans with AD.** CB is abundant in hippocampal neurons, particularly in granule cells of the dentate gyrus and pyramidal cells of the CA1 region (25). Neuronal CB levels were significantly reduced in hAPP<sub>FAD</sub> mice (Figs. 1*A* and 2*B*), primarily in the granular layer of the dentate gyrus and in the molecular layer into which the granule cells extend their dendrites. Pyramidal cells in CA1 and their dendrites in the stratum radiatum were unaffected (Figs. 1*A* and 2*B*). Double-labeling of brain sections from hAPP<sub>FAD</sub> mice for CB and the neuronal marker Neu-N (Fig. 1*B*) indicated that the CB reductions in the dentate gyrus primarily reflected a decrease in neuronal CB levels rather than loss of CB-producing neurons.

Although loss of CB-positive neurons in cortical areas of AD cases has been described (26, 27), we found no studies reporting

CB reductions in granule cells of the dentate gyrus in AD. In fact, granule cells are relatively resistant to AD-associated cell death (28). Yet, we found marked reductions in neuronal CB-IR in the dentate gyrus of AD cases, with the most striking depletions seen in the most severely demented individuals (Fig. 1*D*).

**CB Reductions Depend on Age, A $\beta$ , and Reduced CB mRNA Levels.** CB reduction in hAPP<sub>FAD</sub> mice was age-dependent (Fig. 2*A*). Significant CB reductions in hAPP<sub>FAD</sub> mice were also detected at 6–7, 9–11, and 14–15 mo [ $n$  = 4–8 mice per age and genotype (not shown)]. hAPP mice from line 15, which express hAPP<sub>WT</sub> and have much lower A $\beta$  levels than hAPP<sub>FAD</sub> mice from line J20 (6), had no significant reductions in CB at 6–9 mo (Fig. 2*B* and *C*) or at 11–13 and 13–15 mo (not shown;  $n$  = 8–12 hAPP<sub>WT</sub> mice and  $n$  = 5–11 non-TG controls per age group). Reductions in CB-IR in 6- to 7-mo-old hAPP<sub>FAD</sub> mice correlated tightly with CB protein and mRNA levels in the dentate gyrus of the opposite hemibrain (Fig. 2*C* and *D*), indicating a mechanism affecting gene expression.

**CB Reductions in hAPP<sub>FAD</sub> Mice Are Associated with a Decrease in c-Fos-IR Neurons in the Dentate Gyrus.** The immediate early gene *c-fos* is also critically dependent on calcium (23). The number of c-Fos-IR neurons in the granular layer of the dentate gyrus was significantly reduced in hAPP<sub>FAD</sub> mice even at 4–5 mo of age and decreased further by 6–7 mo (Figs. 1*C* and 2*E* and *F*). Although interindividual variations in CB and c-Fos were substantial (Figs. 1*A* and 3*A*), the reductions were tightly correlated in hAPP<sub>FAD</sub> mice (Fig. 3*A*), suggesting the underlying mechanisms are nonrandom and overlapping.

**Reductions in CB and c-Fos Correlate with Relative Abundance of A $\beta$ 1–42 but Not with Plaque Load or Gender.** At 6–7 mo of age, when CB and c-Fos reductions were prominent, male ( $n$  = 22) and female ( $n$  = 20) hAPP<sub>FAD</sub> mice showed no significant differences ( $P$  > 0.25) in the levels of CB-IR, c-Fos-IR granule cells, and percent area occupied by 3D6-IR A $\beta$  deposits (data not shown). In the dentate gyrus of 6- to 7-mo-old hAPP<sub>FAD</sub> mice ( $n$  = 9), CB mRNA, protein, and IR did not correlate with levels of hAPP<sub>FAD</sub> mRNA or protein ( $P$  > 0.7 for all six CB–hAPP<sub>FAD</sub> correlations, not shown), suggesting that the CB reductions are not caused by the expression of hAPP<sub>FAD</sub> per se.

CB and c-Fos reductions in hAPP<sub>FAD</sub> mice also did not correlate with early A $\beta$  deposition (Fig. 3*B*). When analyzed over a wider age range (4–22 mo), these reductions did not correlate with plaque load either ( $P$  > 0.6). However, they did correlate with A $\beta$ 1–42/A $\beta$ 1–x ratios (Fig. 3*C*), which reflect the abundance of A $\beta$  ending at residue 42 relative to other, mostly shorter, A $\beta$  peptides (29, 30).

**Reductions in CB and c-Fos in the Dentate Gyrus of hAPP<sub>FAD</sub> Mice Correlate Tightly with Deficits in Learning and Memory.** To further assess the pathophysiological significance of CB and c-Fos reductions in hAPP<sub>FAD</sub> mice, we analyzed mice in a Morris water maze test (14), which is widely used to assess learning and memory (31). Behavioral deficits in hAPP<sub>FAD</sub> mice showed a striking relationship to neuronal reductions of CB and c-Fos in the dentate gyrus (Fig. 4).

The majority of hAPP<sub>FAD</sub> mice learned to navigate to a visible platform, demonstrating efficient cued learning (sessions 1–4), but showed significant deficits in the spatial component of the test, during which they had to use extramaze cues to locate a hidden platform in the pool (sessions 5–10) (Fig. 4*A*). These hAPP<sub>FAD</sub> mice were also impaired in the probe trial (Fig. 4*B*), which provides a putative measure of memory retention. In contrast, they did not differ from non-TG controls in swim speed



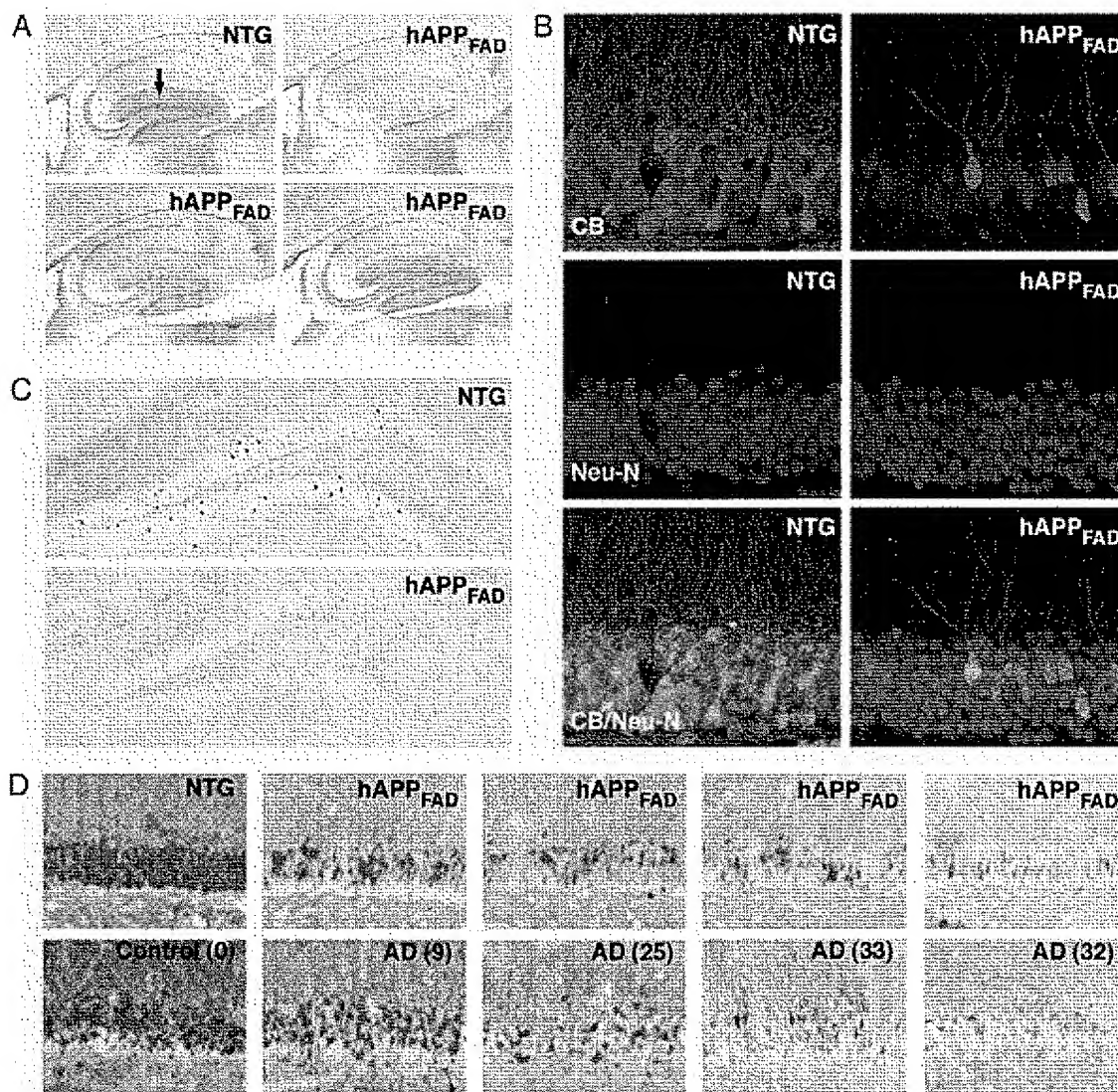


**Fig. 1.** CB and c-Fos reductions in the dentate gyrus of hAPP<sub>FAD</sub> mice and humans with AD. Brain sections from 6- to 7-mo-old mice were immunolabeled for CB, c-Fos, or the neuronal marker Neu-N. (A) Sagittal vibratome sections illustrating typical CB-IR in the dentate gyrus (arrow) of a non-TG mouse and a range of CB reductions in hAPP<sub>FAD</sub> mice. (B) Double-labeling of sagittal vibratome sections for CB (green) and Neu-N (red) did not reveal obvious changes in the density of neuronal nuclei in the CB-depleted granular layer of hAPP<sub>FAD</sub> mice. (C) Coronal sections illustrating the decrease in c-Fos-IR neurons in the granular layer of hAPP<sub>FAD</sub> mice. (D) Hippocampal sections from 6- to 7-mo-old hAPP<sub>FAD</sub> mice (Upper) and AD cases (Lower) were stained for CB. A comparable range of CB reductions was found in the granular layer of hAPP<sub>FAD</sub> mice and AD cases. Numbers in parentheses indicate Blessed score, which increases with the severity of the dementia.

(Fig. 4C), suggesting that their longer escape latencies during the hidden platform sessions were not due to motor deficits.

CB levels in the dentate gyrus did not correlate with cued learning in non-TG mice or in hAPP<sub>FAD</sub> mice with deficits in spatial, but not cued, learning (Fig. 4D). CB levels were also unrelated to performance in the first two sessions of the hidden platform training (Fig. 4E, sessions 5 and 6) before significant spatial learning was evident in non-TG mice (Fig. 4A). However, in hAPP<sub>FAD</sub> mice, CB levels correlated tightly with spatial learning deficits in the last four sessions of hidden platform training (Fig. 4E, sessions 7–10), when spatial learning was clearly evident in non-TG controls (Fig. 4A). This correlation remained strong when escape latencies or path lengths were averaged over all hidden platform trials (Fig. 4F). The relative level of c-Fos-IR granule cells also correlated well with spatial learning in hAPP<sub>FAD</sub> mice but not in non-TG controls (Fig. 4G).

Some hAPP<sub>FAD</sub> mice were excluded from the above analysis because they had significant deficits even in cued learning (Fig. 4H), which confounds the interpretation of deficits in the spatial component of this test (31). These mice had the most prominent reductions in both CB and c-Fos-IR granule cells (Fig. 4I).

## Discussion

Our study demonstrates a cause–effect relationship between the expression of hAPP<sub>FAD</sub>/A $\beta$  and age-dependent reductions in CB and c-Fos in a neuronal population critically involved in learning and memory. Reductions in these calcium-dependent proteins in granule cells of the dentate gyrus correlated tightly with spatial learning deficits in hAPP<sub>FAD</sub> mice and depended on the relative abundance of A $\beta$ 1–42 but not on the amount of A $\beta$  deposited in plaques.

These findings support the hypothesis that AD-related neuronal deficits are caused by small nonfibrillar A $\beta$  assemblies rather than



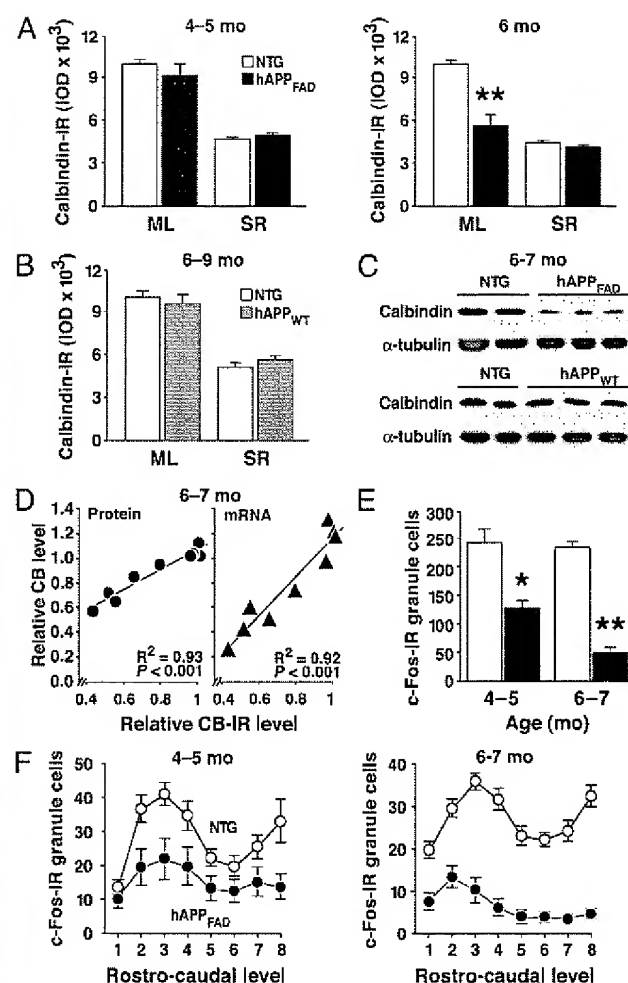


**Fig. 2.** CB and c-Fos reductions in the dentate gyrus depend on age and type of hAPP expressed. (A and B) Coronal brain sections were obtained from hAPP<sup>FAD</sup> mice, hAPP<sup>WT</sup> mice, and non-TG controls (NTG). Ages in months (mo) are indicated (Top) ( $n = 10$ –13 mice per age and genotype). IOD, integrated optical density; ML, molecular layer; SR, stratum radiatum. (C and D) Total protein and RNA were extracted from dentate gyrus samples. Levels of CB protein (C and D Left) and mRNA (D Right) were determined by Western blot analysis and quantitative fluorogenic RT-PCR, respectively. Values obtained in different hAPP<sup>FAD</sup> mice were expressed as CB/ $\alpha$ -tubulin (D Left) and CB/GAPDH (D Right) ratios. (E and F) The relative number of c-Fos-IR neurons in the granular layer was determined in coronal sections from hAPP<sup>FAD</sup> mice (black columns and dots) and non-TG controls (empty columns and dots) ( $n = 13$ –18 mice per age and genotype). Data represent group means for all sections analyzed (E) or for different rostrocaudal levels of the dentate gyrus (F). \*,  $P < 0.05$ ; \*\*,  $P < 0.001$ .

by plaques (4, 6, 8, 14, 15). Although A $\beta$  production depends on hAPP levels, the formation of neurotoxic A $\beta$  assemblies may be influenced by many other variables including the A $\beta$ 1–42/A $\beta$ 1–40 ratio and interindividual differences in the level or activity of proteins that bind or degrade A $\beta$  (32–34). This may explain why reductions in CB and c-Fos in hAPP<sup>FAD</sup> mice correlated with the relative abundance of A $\beta$ 1–42 but not with hAPP<sup>FAD</sup> levels.

Although the exact mechanisms by which A $\beta$  assemblies may reduce CB and c-Fos levels in granule cells remain to be determined, they might involve alterations in the function of calcium channels and other membrane proteins, chronic inflammation, and formation of pores in cell membranes, both in the dentate gyrus and in regions projecting to it (6, 21, 35–41).

The behavioral testing of mice is time consuming, and test results obtained in different laboratories can vary (42, 43). Plaque load is

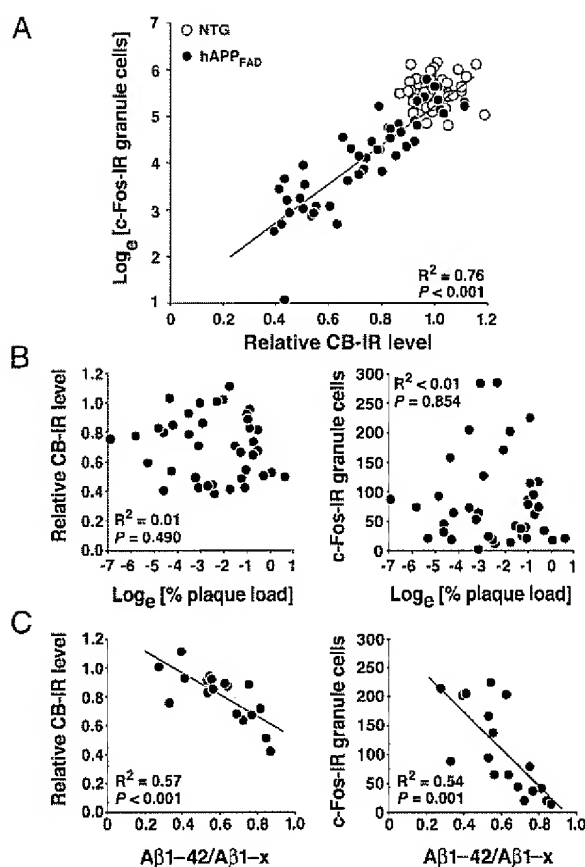


**Fig. 3.** Relationship among CB, c-Fos, plaque load, and A $\beta$  levels. Brain sections and hippocampi were from hAPP<sup>FAD</sup> mice (black dots) and non-TG controls (empty dots). The square of correlation coefficients ( $R^2$ ) and  $P$  values refer to hAPP<sup>FAD</sup> mice only. (A) Relative levels of CB and c-Fos-IR granule cells in the dentate gyrus were strongly correlated in hAPP<sup>FAD</sup> mice but not in non-TG controls ( $n = 48$ –60 per genotype; age, 4–7 mo). (B) Levels of CB and c-Fos-IR granule cells did not correlate with hippocampal plaque load in hAPP<sup>FAD</sup> mice with early plaque formation ( $n = 39$ ; age, 4–7 mo). (C) Hippocampal levels of A $\beta$ 1–42 and A $\beta$ 1–x (approximates total A $\beta$ ) were determined by ELISA as described (6, 29) in hAPP<sup>FAD</sup> mice ( $n = 18$  females) over a wider range of ages (4–22 months; mean  $\pm$  SD, 10.7  $\pm$  6.7 mo).

the most widely used pathological outcome measure in the pre-clinical assessment of anti-A $\beta$  treatments (9–13), although it does not appear to correlate with behavioral deficits (8, 13, 44). Our study suggests that biochemical and radiological measures reflecting CB levels in the dentate gyrus could improve the assessment of AD treatments by providing a more reliable surrogate marker of A $\beta$ -induced neuronal dysfunction.

Some hAPP<sup>FAD</sup> mice have impairments not only in the spatial but also in the cued component of the water maze test (8) (Fig. 4H and I). The mechanisms underlying these impairments might differ from those causing more selective spatial learning deficits quantitatively, qualitatively, or both. The visible and hidden platform components of the water maze test can involve overlapping cognitive functions (7). Extensions of deficits from one component to the other might have been fostered here by the visibility of extramaze cues and the small size of the marker indicating the platform location during cued trials (see *Supporting Text*), which could promote engagement of spatial learning mechanisms. Furthermore, AD affects many brain regions besides the hippocampus, combining spatial learning deficits with other cognitive impairments. Widespread neuronal expression

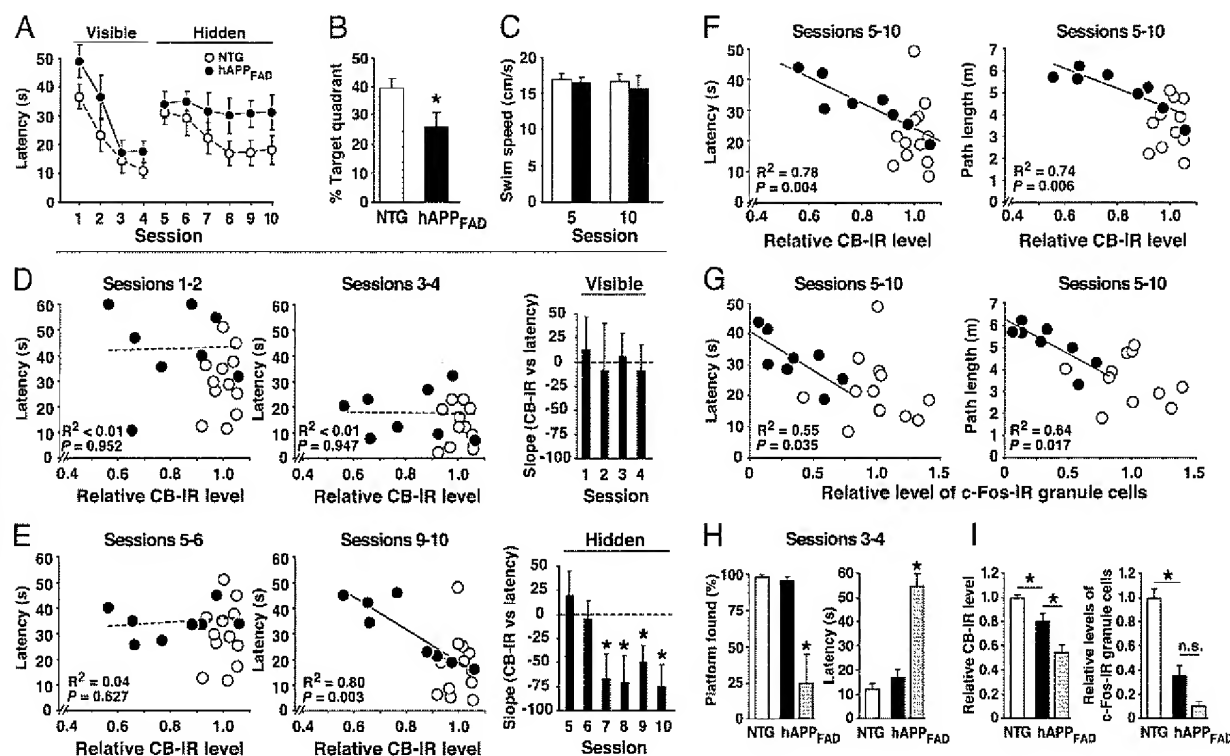


**Fig. 4.** Reductions in CB and c-Fos correlate tightly with behavioral deficits. hAPP<sub>FAD</sub> mice (black dots or columns) and non-TG littermate controls (empty dots and columns) (age 6–7 mo, all males) were trained in a Morris water maze. After behavioral testing, relative levels of CB and c-Fos-IR neurons in the dentate gyrus were measured. (A–C) Learning curves (A), probe trial performance (B), and average swim speeds (C) of non-TG controls ( $n = 12$ ) and of hAPP<sub>FAD</sub> mice ( $n = 8$ ) showing learning deficits when the platform was hidden but not when it was visible. Assessment of session effects in A by repeated-measures ANOVA revealed that hAPP<sub>FAD</sub> mice learned the cued task ( $P < 0.001$ ) but not the spatial task ( $P > 0.95$ ), whereas non-TG controls learned both tasks ( $P < 0.001$ ). Average swim speeds in C were calculated for sessions 5 and 10 from all trials performed in the respective session. (D and E) Relationship of relative CB-IR levels and escape latencies during sessions in which the platform was visible (D) or hidden (E). See A for sequence of sessions. Filled and open circles represent mean latency values of individual mice calculated from the indicated sessions. Bars represent the slope coefficient “ $b$ ” in the linear regression equation ( $y = a + bx$ ) for hAPP<sub>FAD</sub> mice in the training sessions indicated. (F) Correlation of relative CB levels with average escape latencies (Left) and path lengths (Right) calculated from all sessions of hidden platform training. CB levels did not correlate with average swim speeds in the visible ( $P = 0.86$ ) or hidden ( $P = 0.47$ ) platform component of the test. (G) Correlation of relative levels of c-Fos-IR granule cells with average escape latencies (Left) and path lengths (Right) calculated as in F. The mean number of c-Fos-IR granule cells identified in non-TG controls was arbitrarily defined as 1.0. (H) Four hAPP<sub>FAD</sub> mice (gray columns) were excluded from the above analysis, because they showed a significant deficit in the visible platform training, defined here as an average latency (mean of all trials in sessions 3 and 4) exceeding the average latency plus two SD in non-TG controls. In contrast to the other mice, this group of hAPP<sub>FAD</sub> mice did not consistently find the visible platform. (I) Relative levels of CB and c-Fos-IR granule cells in non-TG controls and hAPP<sub>FAD</sub> mice that did or did not show deficits in the visible platform training. \*,  $P < 0.05$ .  $R^2$  and  $P$  values in (D–G) refer to hAPP<sub>FAD</sub> mice only; no significant correlations were identified in non-TG controls.

of hAPP<sub>FAD</sub>/A $\beta$  may have similar effects in severely impaired TG mice.

Our results demonstrate that neuronal populations resisting cell death in AD (28) can still be drastically altered at the molecular level. The marked reduction of CB in the dentate gyrus of patients with sporadic AD demonstrates that FAD mutations are not necessary for such reductions to occur in the human condition. A $\beta$ 42/A $\beta$ 40 ratios high enough to elicit CB reductions within 6 mo may be attainable in hAPP mice only by the introduction of FAD mutations, whereas A $\beta$ 42/A $\beta$ 40 ratios in sporadic AD may be high enough to deplete CB levels over time even in the absence of FAD mutations. More cases will need to be analyzed to establish the extent to which CB reductions correlate with cognitive deficits in AD.

Although it is likely that diverse molecular alterations contribute to AD-associated neuronal dysfunction, the tight association between molecular and functional alterations we identified raises the question of whether reductions in CB and c-Fos not only indicate but also mediate hAPP<sub>FAD</sub>/A $\beta$ -dependent behavioral deficits. Because CB can protect neurons against A $\beta$ -induced toxicity (45), the reduction of CB by A $\beta$  could be part of a vicious cycle promoting progressive neuronal dysfunction in hAPP<sub>FAD</sub> mice and in AD.

Inhibiting CB expression impaired water maze learning in TG mice (46) and prolonged increases in intraneuronal calcium after stimulation of hippocampal slices (36). Ablation of CB also worsened neuronal deficits in a TG model of spinocerebellar ataxia-1 (47), another neurodegenerative disease with abnormal protein accumulation. Ablation or inhibition of c-Fos elicited deficits in the water maze test and related tasks (23, 48).

These findings suggest that reductions in CB and c-Fos in hAPP<sub>FAD</sub> mice and humans with AD may not only reflect cognitive deficits but may contribute to them. The roles of these and related molecular alterations as potential indicators and mediators of neurodegenerative disease merit further investigation.

We thank Hilda Ordoña, Kristina Shockley, and Anthony LeFevour for excellent technical support; Christian Essrich for contributing RT-PCR data; Gary Howard and Stephen Ordway for editorial review; and Denise McPherson for administrative assistance. This work was supported by National Institutes of Health Grants AG11385, NS43945, and NS41787 (to L.M.) and by fellowships from the Spanish Ministry of Education, Culture, and Sport (to J.J.P.) and the John Douglas French Alzheimer's Foundation (to J.C.).

1. Cowan, W. M. & Kandel, E. R. (2001) *J. Am. Med. Assoc.* **285**, 594–600.
2. Games, D., Adams, D., Alessandrini, R., Barbour, R., Berthelette, P., Blackwell, C., Carr, T., Clemens, J., Donaldson, T., Gillespie, F., et al. (1995) *Nature* **373**, 523–527.
3. Dodart, J. C., Meziane, H., Mathis, C., Bales, K. R., Paul, S. M. & Ungerer, A. (1999) *Behav. Neurosci.* **113**, 982–990.
4. Hsia, A., Masliah, E., McConlogue, L., Yu, G., Tatsuno, G., Hu, K., Kholodenko, D., Malenka, R. C., Nicoll, R. A. & Mucke, L. (1999) *Proc. Natl. Acad. Sci. USA* **96**, 3228–3233.
5. Moechars, D., Dewachter, I., Lorent, K., Reverse, D., Baekelandt, V., Naidu, A., Tessier, I., Spittaels, K., Van Den Haute, C., Checler, F., et al. (1999) *J. Biol. Chem.* **274**, 6483–6492.
6. Mucke, L., Masliah, E., Yu, G.-Q., Mallory, M., Rockenstein, E. M., Tatsuno, G., Hu, K., Kholodenko, D., Johnson-Wood, K. & McConlogue, L. (2000) *J. Neurosci.* **20**, 4050–4058.
7. Arendash, G. W. & King, D. L. (2002) *Physiol. Behav.* **75**, 643–652.
8. Westerman, M. A., Cooper-Blacketer, D., Mariash, A., Kotilinek, L., Kawarabayashi, T., Younkin, L. H., Carlson, G. A., Younkin, S. G. & Ashe, K. H. (2002) *J. Neurosci.* **22**, 1858–1867.
9. Cherny, R. A., Atwood, C. S., Xilinas, M. E., Gray, D. N., Jones, W. D., McLean, C. A., Barnham, K. J., Volitakis, I., Fraser, F. W., Kim, Y. S., et al. (2001) *Neuron* **30**, 665–676.
10. Lim, G. P., Yang, F., Chu, T., Gahtan, E., Ubeda, O., Beech, W., Overmier, J. B., Hsiao-Ashe, K., Frautschi, S. A. & Cole, G. M. (2001) *Neurobiol. Aging* **22**, 983–991.
11. McLaurin, J., Cecal, R., Kierstead, M. E., Tian, X., Phinney, A. L., Manca, M., French, J. E., Lambermon, M. H. L., Darabie, A. A., Brown, M. E., et al. (2002) *Nat. Med.* **8**, 1263–1269.
12. Schenk, D. (2002) *Nature* **3**, 824–828.
13. Dodart, J. C., Bales, K. R., Gannon, K. S., Greene, S. J., DeMattos, R. B., Mathis, C., DeLong, C. A., Wu, S., Wu, X., Holtzman, D. M., et al. (2002) *Nat. Neurosci.* **5**, 452–457.
14. Raber, J., Wong, D., Yu, G.-Q., Buttini, M., Mahley, R. W., Pitas, R. E. & Mucke, L. (2000) *Nature* **404**, 352–354.
15. Klein, W. L., Krafft, G. A. & Finch, C. E. (2001) *Trends Neurosci.* **24**, 219–224.
16. Buttini, M., Yu, G.-Q., Shockley, K., Huang, Y., Jones, B., Masliah, E., Mallory, M., Yeo, T., Longo, F. M. & Mucke, L. (2002) *J. Neurosci.* **22**, 10539–10548.
17. Braak, H. & Braak, E. (1998) *J. Neural Transm.* **105**, Suppl. 53, 127–140.
18. Thal, D. R., Rüb, U., Orantes, M. & Braak, H. (2002) *Neurology* **58**, 1791–1800.
19. Burgess, N., Maguire, E. A. & O'Keefe, J. (2002) *Neuron* **35**, 625–641.
20. Berridge, M. J. (1998) *Neuron* **21**, 13–26.
21. Mattson, M. P. & Chan, S. L. (2001) *J. Mol. Neurosci.* **17**, 205–224.
22. Carafoli, E. (2002) *Proc. Natl. Acad. Sci. USA* **99**, 1115–1122.
23. Guzowski, J. F. (2002) *Hippocampus* **12**, 86–104.
24. Rockenstein, E. M., McConlogue, L., Tan, H., Gordon, M., Power, M., Masliah, E. & Mucke, L. (1995) *J. Biol. Chem.* **270**, 28257–28267.
25. Celio, M. R. (1990) *Neuroscience* **35**, 375–475.
26. Ichimiya, Y., Emson, P. C., Mountjoy, C. Q., Lawson, D. E. M. & Heizmann, C. W. (1988) *Brain Res.* **475**, 156–159.
27. Hof, P. R. & Morrison, J. H. (1991) *Exp. Neurol.* **111**, 293–301.
28. West, M. J., Coleman, P. D., Flood, D. G. & Troncoso, J. C. (1994) *Lancet* **344**, 769–772.
29. Johnson-Wood, K., Lee, M., Motter, R., Hu, K., Gordon, G., Barbour, R., Khan, K., Gordon, M., Tan, H., Games, D., et al. (1997) *Proc. Natl. Acad. Sci. USA* **94**, 1550–1555.
30. Gouras, G. K., Xu, H., Jovanovic, J. N., Buxbaum, J. D., Wang, R., Greengard, P., Reikun, N. R. & Gandy, S. (1998) *J. Neurochem.* **71**, 1920–1925.
31. D'Hooge, R. & De Deyn, P. P. (2001) *Brain Res. Rev.* **36**, 60–90.
32. Lambert, M. P., Barlow, A. K., Chromy, B. A., Edwards, C., Freed, R., Liosatos, M., Morgan, T. E., Rozovsky, I., Trommer, B., Viola, K. L., et al. (1998) *Proc. Natl. Acad. Sci. USA* **95**, 6448–6453.
33. Seikoe, D. J. (2001) *Neuron* **32**, 177–180.
34. Stine, W. B., Jr., Dahlgren, K. N., Krafft, G. A. & LaDu, M. J. (2003) *J. Biol. Chem.* **278**, 11612–11622.
35. Heyser, C. J., Masliah, E., Samimi, A., Campbell, I. L. & Gold, L. H. (1997) *Proc. Natl. Acad. Sci. USA* **94**, 1500–1505.
36. Pasti, L., Carmignoto, G., Pozzan, T., Battini, R., Ferrari, S., Lally, G. & Emson, P. C. (1999) *NeuroReport* **10**, 2367–2372.
37. Nägeli, U. V., Mody, I., Jeub, M., Lie, A. A., Elger, C. E. & Beck, H. (2000) *J. Neurosci.* **20**, 1831–1836.
38. Dineley, K. T., Westerman, M., Bui, D., Bell, K., Ashe, K. H. & Sweatt, J. D. (2001) *J. Neurosci.* **21**, 4125–4133.
39. Lin, H., Bhatia, R. & Lal, R. (2001) *FASEB J.* **15**, 2433–2444.
40. Wyss-Coray, T. & Mucke, L. (2002) *Neuron* **35**, 419–432.
41. Redwine, J. M., Kosofsky, B., Jacobs, R. E., Games, D., Reilly, J. F., Morrison, J. H., Young, W. G. & Bloom, F. E. (2003) *Proc. Natl. Acad. Sci. USA* **100**, 1381–1386.
42. Crabbe, J. C., Wahlsten, D. & Dudek, B. C. (1999) *Science* **284**, 1670–1672.
43. Wahlsten, D., Metten, P., Phillips, T. J., Boehm, S. L., II, Burkhart-Kasch, S., Dorow, J., Doerksen, S., Downing, C., Fogarty, J., Rodd-Henricks, K., et al. (2003) *J. Neurobiol.* **54**, 283–311.
44. Holcomb, L. A., Gordon, M. N., Jantzen, P., Hsiao, K., Duff, K. & Morgan, D. (1999) *Behav. Genet.* **29**, 177–185.
45. Guo, Q., Christakos, S., Robinson, N. & Mattson, M. P. (1998) *Proc. Natl. Acad. Sci. USA* **95**, 3227–3232.
46. Molinari, S., Battini, R., Ferrari, S., Pozzi, L., Killcross, A. S., Robbins, T. W., Jouvenceau, A., Billard, J.-M., Dutar, P., Lamour, Y., et al. (1996) *Proc. Natl. Acad. Sci. USA* **93**, 8028–8033.
47. Vig, P. J. S., Subramony, S. H. & McDaniel, D. O. (2001) *Brain Res. Bull.* **56**, 221–225.
48. He, J., Yamada, K. & Nabeshima, T. (2002) *Neuropsychopharmacology* **26**, 259–268.

# Vulnerability of Dentate Granule Cells to Disruption of Arc Expression in Human Amyloid Precursor Protein Transgenic Mice

Jorge J. Palop,<sup>1,2</sup> Jeannie Chin,<sup>1,2</sup> Nga Bien-Ly,<sup>1</sup> Catherine Massaro,<sup>1,3</sup> Bertrand Z. Yeung,<sup>1</sup> Gui-Qiu Yu,<sup>1</sup> and Lennart Mucke<sup>1,2,3</sup>

<sup>1</sup>Gladstone Institute of Neurological Disease, <sup>2</sup>Department of Neurology, and <sup>3</sup>Neuroscience Graduate Program, University of California, San Francisco, San Francisco, California 94158

Activity-induced expression of *Arc* is necessary for maintenance of long-term potentiation and for memory consolidation. In transgenic (TG) mice with neuronal production of human amyloid precursor protein (hAPP) and hAPP-derived amyloid- $\beta$  (A $\beta$ ) peptides, basal *Arc* expression was reduced primarily in granule cells of the dentate gyrus. After exploration of a novel environment, *Arc* expression in these neurons was unaltered in hAPP mice but increased markedly in nontransgenic controls. Other TG neuronal populations showed no or only minor deficits in *Arc* expression, indicating a special vulnerability of dentate granule cells. The phosphorylation states of NR2B and ERK1/2 were reduced in the dentate gyrus of hAPP mice, suggesting attenuated activity in NMDA-dependent signaling pathways that regulate synaptic plasticity as well as *Arc* expression. *Arc* reductions in hAPP mice correlated with reductions in the actin-binding protein  $\alpha$ -actinin-2, which is located in dendritic spines and, like *Arc*, fulfills important functions in excitatory synaptic activity. Reductions in *Arc* and  $\alpha$ -actinin-2 correlated tightly with reductions in Fos and calbindin, shown previously to reflect learning deficits in hAPP mice. None of these alterations correlated with the extent of plaque formation, suggesting a plaque-independent mechanism of hAPP/A $\beta$ -induced neuronal deficits. The brain region-specific depletion of factors that participate in activity-dependent modification of synapses may critically contribute to cognitive deficits in hAPP mice and possibly in humans with Alzheimer's disease.

**Key words:** Alzheimer; dendritic spines; immediate-early gene; NMDA; novel environment; plasticity

## Introduction

Alzheimer's disease (AD) results in progressive impairment of memory consolidation. Memory retrieval is also affected in a characteristic pattern, in which recent memories are more vulnerable than older memories (Eustache et al., 2004; Sadek et al., 2004). These impairments suggest an early vulnerability of the hippocampus and a subsequent disruption of neocortical networks sustaining consolidated memories (Wiltgen et al., 2004). Although the differential loss of neurons in specific brain regions in AD has been mapped carefully (Braak and Braak, 1991; West et al., 1991; Corder et al., 2000), little is known about the neuronal populations that first become dysfunctional, and even less about the underlying molecular mechanisms. Understanding the processes that cause neuronal dysfunction in AD and related models could guide the development of treatments to prevent AD, pre-

serve learning and memory in its early stages, and maximize cognitive functions in the later stages of the illness.

Transgenic (TG) mouse models with neuronal production of human amyloid precursor protein (hAPP) and hAPP-derived amyloid- $\beta$  (A $\beta$ ) peptides develop a range of AD-like alterations, including age-dependent deficits in learning and memory (Higgins and Jacobsen, 2003; Walsh and Selkoe, 2004; Kobayashi and Chen, 2005). However, the cellular and molecular substrates of these cognitive deficits remain to be identified. Our previous analysis of hAPP mice (Palop et al., 2003) and reports by others (Dickey et al., 2003, 2004) suggested that the depletion of synaptic activity-dependent proteins may play a critical role in A $\beta$ -induced cognitive decline. Particularly intriguing to us in this context were alterations in the immediate-early gene product *Arc* (activity-regulated cytoskeleton-associated protein), the expression of which has been used previously to image cellular networks involved in encoding of contextual information (Guzowski et al., 1999; Burke et al., 2005).

*Arc* is expressed predominantly in cortical and hippocampal glutamatergic neurons; it is required for maintenance of long-term potentiation (LTP) and for memory consolidation (Lyford et al., 1995; Guzowski et al., 2000; Steward and Worley, 2001). Stimulated neurons rapidly increase *Arc* mRNA expression, which allows for the identification of neuronal network activity (Lyford et al., 1995; Guzowski et al., 1999; Temple et al., 2003;

Received March 14, 2005; revised Aug. 15, 2005; accepted Aug. 17, 2005.

This work was supported in part by National Institutes of Health Grants AG023501, AG11385, AG022074, and NS41787 to L.M. We thank S. Chowdhury and P. F. Worley for the full-length mouse *Arc* cDNA clone and the *Arc* antibody; P. Seubert and L. McConlogue for the 3D6 antibody; I. Cobos for advice on *in situ* hybridization; X. Wang and H. Ordozua for technical support; S. Finkbeiner, S. Mitra, and V. Rao for helpful comments on this manuscript; G. Howard and S. Ordway for editorial review; and D. McPherson and L. Manuntag for administrative assistance.

Correspondence should be addressed to Dr. Lennart Mucke, Gladstone Institute of Neurological Disease, 1650 Owens Street, San Francisco, CA 94158. E-mail: lmucke@gadstone.ucsf.edu.

DOI:10.1523/JNEUROSCI.2829-05.2005

Copyright © 2005 Society for Neuroscience 0270-6474/05/259686-08\$15.00/0

Vazdarjanova and Guzowski, 2004). Furthermore, *Arc* mRNA is induced in activated neuronal ensembles in the hippocampus that respond to specific environments, providing a potential network mechanism for encoding spatial and contextual information (Guzowski et al., 1999; Vazdarjanova and Guzowski, 2004).

To further elucidate the role of *Arc* and related factors in hAPP/ $\text{A}\beta$ -induced neuronal deficits *in vivo*, we studied hAPP TG mice that have high levels of  $\text{A}\beta$  in the hippocampus and neocortex and that develop age-related synaptic deficits as well as impairments in learning and memory (Hsia et al., 1999; Mucke et al., 2000; Palop et al., 2003). We monitored *Arc* expression in their brains at baseline and after behavioral or pharmacological stimulation to determine whether  $\text{A}\beta$  affects *Arc* expression differentially in different neuronal populations, whether it affects only induced or also basal *Arc* expression, whether the reported block to *Arc* induction can be overcome by pharmacological stimulation of excitatory neurotransmitter receptors, and whether disruption of *Arc* expression depends on the parenchymal deposition of fibrillar  $\text{A}\beta$  in amyloid plaques. We also tested whether *Arc* expression deficits may be linked to deficits in other synaptic plasticity-related factors, including alterations in the NMDA-mediated signaling pathway.

## Materials and Methods

**TG mice.** We studied 5- to 8-month-old heterozygous TG and nontransgenic (NTG) mice from lines J20 and I5. Line J20 expresses hAPP carrying the Swedish and Indiana FAD (familial AD) mutations (hAPP<sub>FAD</sub>), and line I5 expresses wild-type hAPP (hAPP<sub>WT</sub>) at comparable levels (Mucke et al., 2000). In both lines, neuronal expression of hAPP is directed by the platelet-derived growth factor (PDGF)  $\beta$ -chain promoter. Mice were N<sub>12</sub>–N<sub>15</sub> offspring from crosses between heterozygous TG mice and C57BL/6J NTG breeders. Gender had no detectable effect on any of the parameters analyzed (data not shown). All experiments were approved by the Committee on Animal Research of the University of California, San Francisco.

**Novel environment.** Four to 5 d before the experiment, female mice were pair-housed (one hAPP<sub>FAD</sub> mouse and one NTG control per cage), whereas male mice were singly housed. Mice assigned to novel environment exploration were then transferred to a larger cage (45 × 25 × 20 cm) in an adjacent room. The new room differed markedly in size, shape, light, and furnishing. The new cage was uncovered and contained different bedding and five novel objects. The mice were allowed to explore the new environment for 2 h; the remaining mice stayed undisturbed in their home cages.

The activity (ambulatory movements, rearing, sniffing, digging) of the mice and their interactions with the novel objects were quantified from video records during the first 10 min of each hour in the new cage. An object-interaction event was defined as any close exploratory activity with any novel object. Observers were blinded to genotype. After the observation period, alternate groups of mice assigned to the home cage or novel environment conditions were taken to an adjacent room, deeply anesthetized, and perfused transcardially.

**Kainate injections.** Kainate (Sigma, St. Louis, MO) was dissolved in PBS to 1.8 mg/ml for intraperitoneal injection. All mice (three TG and three NTG) given injections of 18 mg/kg kainate displayed tonic-clonic seizures starting 10–45 min after the injection. Of 28 mice (16 TG and 12 NTG) given injections of 10 mg/kg kainate, only one TG mouse developed seizure activity and was excluded from additional analyses. All mice were killed 2 h after the injection.

**Tissue preparation.** Anesthetized mice were flush-perfused transcardially with phosphate buffer, followed by 4% phosphate-buffered paraformaldehyde. The brains were removed and drop-fixed with the same fixative at 4°C for 48 h. After rinsing with PBS, brains were transferred to 30% sucrose in PBS at 4°C for 24 h and coronally sectioned with a sliding microtome. Ten subseries of floating sections (30  $\mu\text{m}$ ) were collected per mouse and kept at –20°C in cryoprotectant medium until use. Each subseries contained sections throughout the rostrocaudal extent of the

forebrain. All solutions were prepared with autoclaved water containing 0.1% diethyl pyrocarbonate and filtered (pore size, 0.22  $\mu\text{m}$ ).

**In situ hybridization.** Antisense and sense cRNA probes were generated from a linearized plasmid containing full-length *Arc* cDNA (~3 kbp) with T7 and T3 polymerase (Promega, Madison, WI) and premixed RNA-labeling nucleotide mixes containing digoxigenin (Roche Molecular Biochemicals, Palo Alto, CA). The yield and integrity of cRNA riboprobes was confirmed by gel electrophoresis. *In situ* hybridization was performed on floating coronal sections (30  $\mu\text{m}$ ). After removing cryoprotectant medium with PBS, floating sections were fixed in 4% buffered paraformaldehyde, treated with 0.005% proteinase K in Tris-HCl, pH 8.0, EDTA, and 0.5% Tween for 15 min, and incubated with 1.335% triethanolamine, 0.175% HCl, and 0.25% acetic anhydride for 10 min. Between steps, sections were washed three times with PBS and 0.5% Tween at room temperature. Sections were then incubated with prehybridization buffer containing 50% formamide, 5× SSC, 5× Denhardt's solution, salmon sperm DNA, and yeast tRNA for 4–6 h at room temperature. Riboprobes were diluted in the prehybridization buffer, heated to 70°C, and added to the sections. Hybridization was done at 67°C for 16 h. Hybridized sections were washed once with 5× SSC, followed by washes in 0.2× SSC at 67°C for 4 h. Sections were transferred to Tris, saline, and 0.5% Tween buffer, blocked with 10% heat-inactivated sheep serum, and incubated overnight with sheep anti-digoxigenin-alkaline phosphatase (1:5000; Roche Molecular Biochemicals). Finally, nitroblue tetrazolium/5-bromo-4-chloro-3-indolyl phosphate (1:50; Roche Molecular Biochemicals) in NTMT (100 mM NaCl, 100 mM Tris-HCl, pH 9.5, 50 mM MgCl<sub>2</sub>, 0.1% Triton X-100) buffer was used to visualize the signal. No signal was detected when sense *Arc* riboprobe was used (data not shown).

**Immunohistochemistry.** Microtome sections (30  $\mu\text{m}$ ) were stained with the standard avidin-biotin/oxidase method. Briefly, after quenching endogenous peroxidase activity and blocking nonspecific binding, sections were incubated with rabbit anti-Arc (1:8000; a gift from S. Chowdhury and P. F. Worley, Johns Hopkins University School of Medicine, Baltimore, MD), rabbit anti-calbindin (1:15,000; Swant, Bellinzona, Switzerland), mouse anti- $\alpha$ -actinin-2 (1:10,000; Sigma), or biotinylated mouse anti-A $\beta$  (1:500, 3D6; Elan Pharmaceuticals, South San Francisco, CA) antibody. Nonbiotinylated primary antibodies were detected with biotinylated goat anti-rabbit (1:200; Vector Laboratories, Burlingame, CA) or donkey anti-mouse (1:500; Jackson ImmunoResearch, West Grove, PA) antibody. Diaminobenzidine was the chromogen.

**Quantitative analysis of brain sections.** *Arc* mRNA and *Arc* immunoreactivity (IR) were quantitated as described previously (Temple et al., 2003). Heavily labeled *Arc*-expressing cells in the granular layer were counted in every 10th section throughout the rostrocaudal extent of this layer with a 20× objective by an investigator blinded to genotype and treatment. Results are presented as the total number of positive cells counted per hemibrain. For each mouse, closely matching results were obtained in the opposite hemibrain (data not shown). Quantitations were confirmed by two independent experimenters (data not shown).

The relative levels of *Arc* mRNA and *Arc* IR in the CA1 pyramidal layer, CA1 stratum radiatum, and neocortex (primary somatosensory cortex) were quantitated by measuring the integrated optical density (IOD) in three sections (30  $\mu\text{m}$  thick, 300  $\mu\text{m}$  apart) between –1.70 and –2.80 mm from bregma with the BioQuant Image Analysis System (R&M Biometrics, Nashville, TN). Two IOD measurements per region and section were taken. The intensity of *Arc* mRNA labels in NTG mice removed directly from their home cage was defined as 1. Relative levels of *Arc* IR were obtained by determining in each section the ratio between IOD values in the region of interest and IOD values in the thalamus (background IR). *Arc* expression in the respective regions of other mice was expressed relative to this baseline. IRs for calbindin,  $\alpha$ -actinin-2, Fos, and A $\beta$  (plaque load) were quantified as described previously (Palop et al., 2003).

**Western blot analysis.** A McIlwain tissue chopper was used to cut hemibrains into 450- $\mu\text{m}$ -thick horizontal sections from which the dentate gyrus was microdissected on ice. For protein quantifications, dentate gyrus samples from each hemibrain were pooled and homogenized on ice in buffer containing 320 mM sucrose, 10 mM Tris-HCl, pH 7.4, 10 mM EDTA, 10 mM EGTA, 1% deoxycholate, protease inhibitor mixture



(Roche Molecular Biochemicals), and phosphatase inhibitor mixtures I and II (Sigma). Samples were then briefly sonicated on ice and centrifuged at  $5000 \times g$  for 10 min. Equal amounts of protein (determined by the Bradford assay) were resolved by SDS-PAGE on 4–12% gradient gels and transferred to nitrocellulose membranes. For analysis of phosphoproteins, membranes were labeled with anti-pY1472 antibody (1:1000 rabbit polyclonal; Chemicon, Temecula, CA) or anti-dually phosphorylated extracellular signal-regulated kinase 1/2 (ERK1/2; 1:2500 rabbit polyclonal; Cell Signaling, Beverly, MA), followed by incubation with HRP-conjugated goat anti-rabbit IgG (1:5000; Chemicon) secondary antibody. For analysis of total protein levels, blots were stripped and reprobed with anti-NR2B antibody (1:10,000 rabbit polyclonal; Chemicon) or anti-pan-ERK1/2 (1:2,500 rabbit polyclonal; Cell Signaling). Bands were visualized by ECL and quantitated densitometrically with Quantity One 4.0 software (Bio-Rad, Hercules, CA).

**Statistical analysis.** Statistical analyses were performed with SPSS 10.0 (SPSS, Chicago, IL). Differences between means were assessed by unpaired, two-tailed Student's *t* test or by ANOVA, followed by Tukey–Kramer *post hoc* test. Differences between expected and observed frequencies were assessed by  $\chi^2$  test. Correlations were examined by simple regression analysis. Null hypotheses were rejected at the 0.05 level.

## Results

### Brain region-specific decreases in basal and induced *Arc* expression in hAPP<sub>FAD</sub> mice

In NTG controls removed directly from their home cage, basal *Arc* mRNA expression in the forebrain was widespread and relatively uniform in cortical and hippocampal pyramidal neurons but more discrete in the dentate gyrus, where scattered granule cells exhibited high levels of labeling (Fig. 1*A, C*). This expression pattern is consistent with previous reports (Lyford et al., 1995; Temple et al., 2003). Basal *Arc* expression in hAPP<sub>FAD</sub> mice was similar, except for a prominent reduction in *Arc*-expressing granule cells (Figs. 1*A, 2C–F*). It should be noted in this context that the PDGF promoter used in these mice directs widespread neuronal production of hAPP/A $\beta$  in different lines of TG mice (Games et al., 1995; Rockenstein et al., 1995; Mucke et al., 2000).

To determine whether granule cells of hAPP<sub>FAD</sub> mice upregulate *Arc* expression when a new context is encountered, mice were allowed to explore a novel environment for 2 h. In NTG mice, environmental exploration markedly increased *Arc* expression in all regions expressing *Arc* at baseline (Figs. 1*B, C, 2A, C–F*), consistent with previous findings (Temple et al., 2003). In hAPP<sub>FAD</sub> mice, exploration significantly increased *Arc* expression in the CA1 pyramidal layer, CA1 stratum radiatum, and neocortex, but not in granule cells, which showed no evidence of *Arc* induction (Figs. 1*B, 2B, C–F*).

To investigate whether the *Arc* expression deficit in hAPP<sub>FAD</sub>

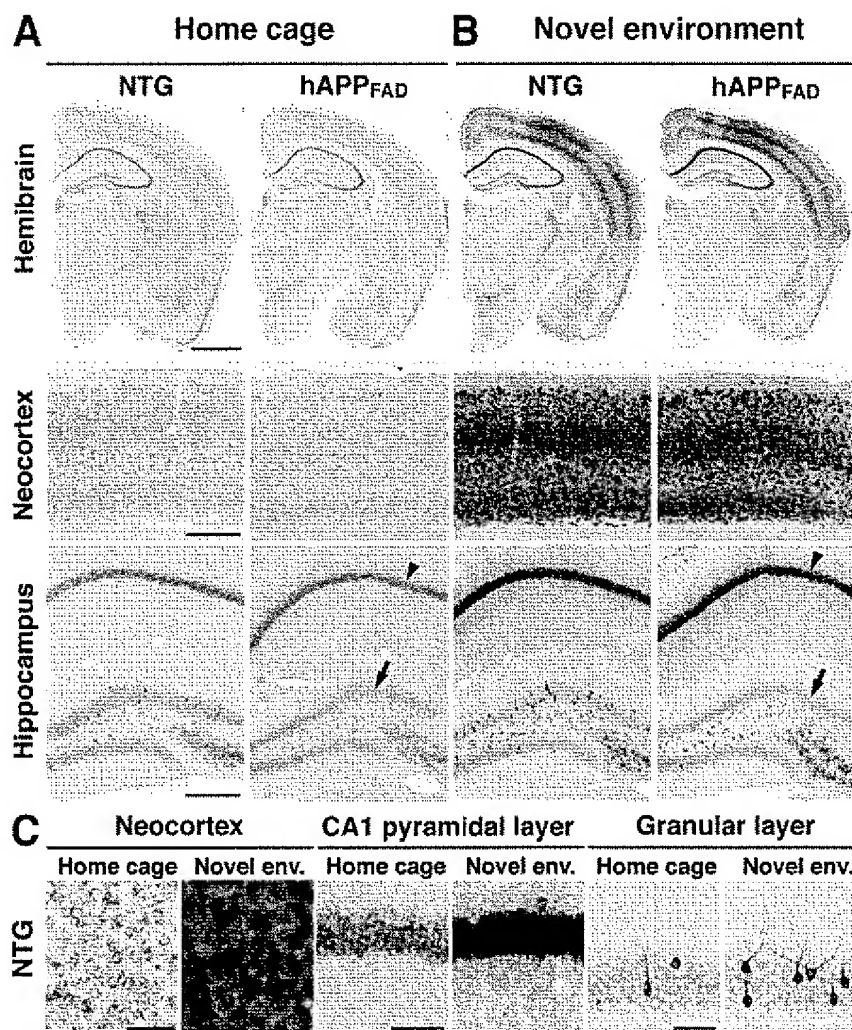


**Figure 1.** Brain region-specific deficits in basal and stimulated *Arc* expression in hAPP<sub>FAD</sub> mice. NTG and TG (hAPP<sub>FAD</sub>) mice were placed into a novel environment or left in their home cage. Two hours later, they were anesthetized and perfused transcardially. *Arc* *in situ* hybridization was performed on floating coronal sections. *A*, Basal *Arc* mRNA levels in the hemibrain, neocortex, and hippocampus of mice maintained in the home cage. *B*, *Arc* mRNA levels in mice that had explored the novel environment. Note the increased *Arc* expression in multiple brain regions, including the CA1 pyramidal layer (arrowhead), after exploration of the novel environment, and the selective decrease in *Arc* expression in the granule cell layer of hAPP<sub>FAD</sub> mice (arrows) under basal (*A*) and stimulated (*B*) conditions. *C*, Higher-magnification images of different brain regions in NTG mice. Novel env., Novel environment. Scale bars: *A, B*, 1 mm (top), 250  $\mu$ m (middle, bottom); *C*, 50  $\mu$ m.

mice was also evident at the protein level, we labeled brain sections with an anti-Arc antibody. Environmental exploration markedly increased Arc IR in cortical and hippocampal areas in NTG mice (Fig. 3). Arc IR was concentrated in neuronal nuclei in mice that explored the novel environment but not in mice that were maintained in the home cage (data not shown). In hAPP<sub>FAD</sub> mice that explored the novel environment, Arc IR levels increased in the pyramidal layer and stratum radiatum of CA1, as well as in the neocortex, but not in the granular layer of the dentate gyrus (Fig. 3*B–F*). Inductions of Arc IR in the CA1 region and the neocortex were similar in magnitude in hAPP<sub>FAD</sub> mice and NTG controls (Fig. 3*D–F*).

To determine whether the granule cell induction of other immediate-early genes was also affected in hAPP<sub>FAD</sub> mice, we examined the expression of Fos. At baseline, hAPP<sub>FAD</sub> mice had fewer Fos-immunoreactive granule cells than NTG controls (Fig. 4*A, C*), consistent with previous observations (Palop et al., 2003).

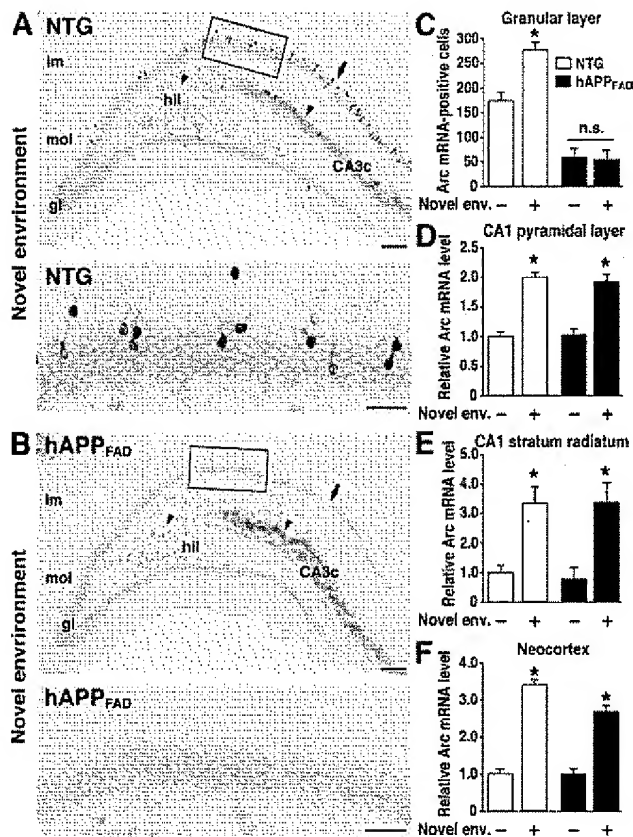


**Figure 2.** Lack of *Arc* induction in granule cells of hAPP<sub>FAD</sub> mice after exploration of a novel environment. *A, B*, *In situ* hybridization illustrates the heterogeneity of *Arc*-expressing cells in the dentate gyrus and the differential susceptibility of distinct neuronal populations to impairments in *Arc* expression in hAPP<sub>FAD</sub> mice. Note the induced *Arc* expression in granule cells (arrow), hilar cells (arrowhead), and proximal CA3c pyramidal cells (arrowhead) in an NTG mouse (*A*) and the selective absence of *Arc* mRNA induction in the granule cells (arrow) of an hAPP<sub>FAD</sub> mouse (*B*). The bottom panels depict higher-magnification images from the squared regions in *A* and *B*. Scale bars: top, 100  $\mu$ m; bottom, 50  $\mu$ m. Im, Stratum lacunosum-moleculare; mol, molecular layer; gl, granular layer; hil, hilus. *C–F*, Quantitation of *Arc* expression at baseline and after exploration of a novel environment (Novel env.). The number of *Arc*-positive granule cells and the optical density of *in situ* hybridization labels in other brain regions were assessed in coronal sections from NTG controls ( $\square$ ) and hAPP<sub>FAD</sub> mice ( $\blacksquare$ ) that had (+) or had not (–) explored a novel environment ( $n = 11–12$  per genotype and condition). hAPP<sub>FAD</sub> mice had significantly fewer *Arc*-positive cells in the granular layer of the dentate gyrus than NTG controls, both at baseline and after exploration (*C*). Basal levels of *Arc* mRNA in the CA1 pyramidal layer (*D*), CA1 stratum radiatum (*E*), and neocortex (*F*) were similar in hAPP<sub>FAD</sub> mice and NTG controls. In both groups, *Arc* mRNA expression in these regions increased robustly after exploration of the novel environment. \* $p < 0.01$  versus home-caged group of the same genotype (Tukey–Kramer test). Error bars indicate SEM. n.s., Nonsignificant.

After environmental exploration, hAPP<sub>FAD</sub> mice showed no increase in the number of Fos-immunoreactive granule cells, whereas NTG mice showed a robust increase (Fig. 4*B,C*). In contrast, Fos induction in the CA1 pyramidal layer was similar in hAPP<sub>FAD</sub> mice and NTG controls (Fig. 4*A,B*). Granule cell levels of Fos and *Arc* expression in hAPP<sub>FAD</sub> mice were tightly correlated both at baseline ( $R^2 = 0.82$ ;  $p < 0.001$ ) and after environmental exploration ( $R^2 = 0.84$ ;  $p < 0.001$ ), suggesting that hAPP<sub>FAD</sub> affects a regulatory mechanism common to different immediate-early genes.

To exclude the possibility that the deficits in *Arc* and Fos induction in hAPP<sub>FAD</sub> mice resulted from deficits in exploratory drive and a consequent lack of sensory stimulation, we monitored the motor activity of mice in the novel environment.

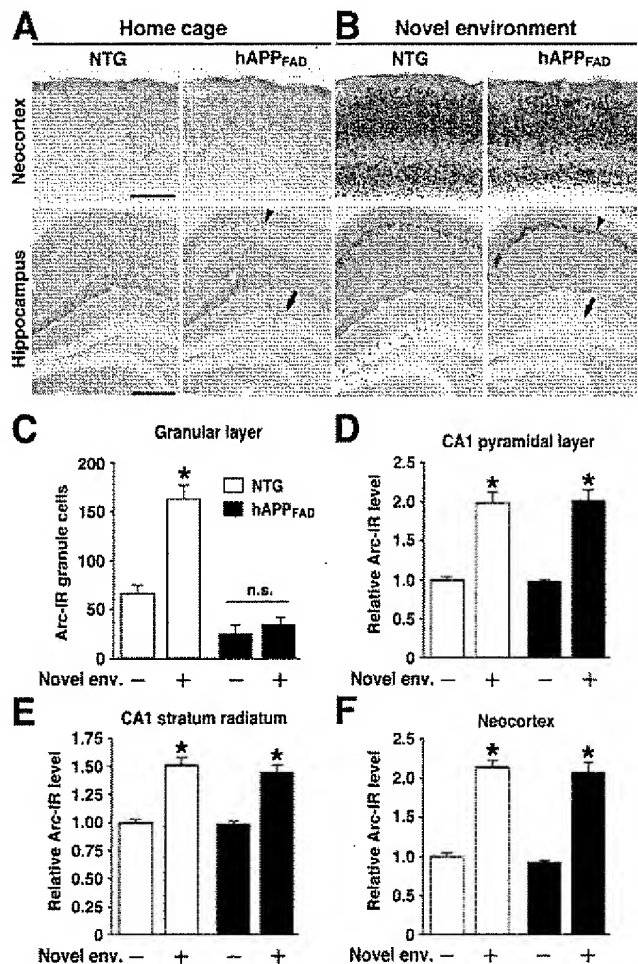


**Figure 3.** Brain region-specific *Arc* expression deficits in hAPP<sub>FAD</sub> mice are also detectable at the protein level. Arc immunostaining was performed on floating coronal sections. *A*, Basal levels of Arc IR in the neocortex and hippocampus of mice maintained in their home cage. *B*, Arc-immunoreactive levels in mice that had explored a new environment. Note the increased Arc expression after environmental exploration in the neocortex and in the CA1 pyramidal layer (arrowheads) and the selective decrease in basal (*A*) and stimulated (*B*) Arc IR in the granular layer of hAPP<sub>FAD</sub> mice (arrows). Scale bars, 250  $\mu$ m. *C–F*, Quantitation of Arc-immunoreactive levels. The number of Arc-immunoreactive granule cells and the optical density of immunolabels in other brain regions were assessed in NTG ( $\square$ ) and hAPP<sub>FAD</sub> ( $\blacksquare$ ) mice that had (+) or had not (–) explored a novel environment (Novel env.;  $n = 11–14$  per genotype and condition). hAPP<sub>FAD</sub> mice had significantly fewer Arc-immunoreactive cells in the granular layer than NTG controls under basal conditions and showed no increase in Arc IR after exploration (*C*). Arc IR in the CA1 pyramidal layer (*D*), CA1 stratum radiatum (*E*), and neocortex (*F*) were similar in hAPP<sub>FAD</sub> mice and NTG controls under both basal and stimulated conditions. \* $p < 0.01$  versus home-caged group of the same genotype (Tukey–Kramer test). Error bars indicate SEM. n.s., Nonsignificant.

hAPP<sub>FAD</sub> mice interacted more with the novel objects than NTG controls (Fig. 4*D*) and were slightly more active in general (data not shown), indicating that they had no deficits in exploratory drive.

#### Resistance of hAPP<sub>FAD</sub> TG granule cells to *Arc* induction can be overcome by kainate-induced seizure activity

To determine whether the deficits in *Arc* induction in granule cells of hAPP<sub>FAD</sub> mice are attributable to a general inability to upmodulate *Arc* expression, we challenged mice with a seizure-inducing dose of kainate (18 mg/kg). After 2 h, *Arc* expression increased markedly in granule cells of both NTG and hAPP<sub>FAD</sub> mice (Fig. 5*A*), indicating that granule cells of both groups can, in



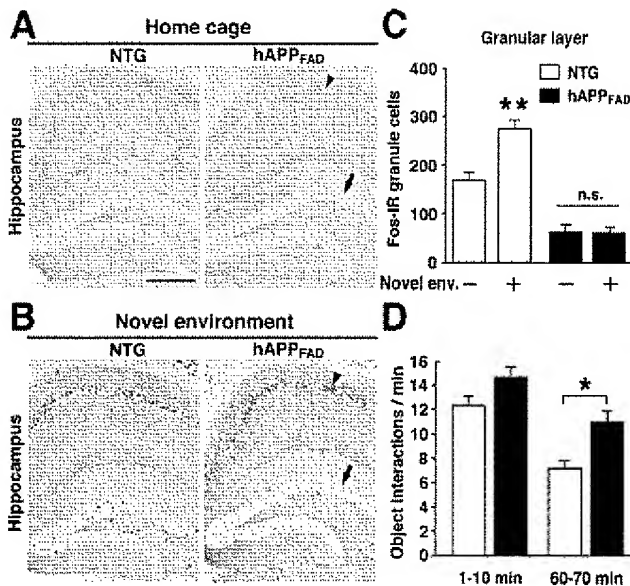


**Figure 4.** Granule cells of hAPP<sub>FAD</sub> mice also fail to increase Fos expression after environmental exploration. **A, B**, Typical patterns of Fos IR in the hippocampus of mice that were kept in their home cage (**A**) or allowed to explore a novel environment (**B**). Note the lack of Fos induction in the granule cells (arrow) and the normal Fos induction in CA1 pyramidal cells (arrowhead) in hAPP<sub>FAD</sub> mice. Scale bar: **A**, 250  $\mu$ m. **C**, The number of Fos-positive granule cells was quantified in NTG (□) and hAPP<sub>FAD</sub> (■) mice that had (+) or had not (–) explored a novel environment (Novel env.;  $n = 17$ –19 per genotype and condition). hAPP<sub>FAD</sub> mice had significantly fewer Fos-immunoreactive cells in the granular layer of the dentate gyrus than NTG controls, both at baseline and after exploration. \*\* $p < 0.01$  versus home-caged group of the same genotype (Tukey–Kramer test). n.s., Nonsignificant. **D**, Object interactions in the novel environment were quantified from video records during two 10 min periods. \* $p < 0.05$  versus NTG (Student's  $t$  test). Error bars indicate SEM. n.s., Nonsignificant.

fact, upmodulate *Arc* expression in response to this type of coordinated network stimulation.

To test whether hAPP<sub>FAD</sub> mice have an increased threshold for kainate-mediated *Arc* induction, we challenged NTG and hAPP<sub>FAD</sub> mice with a lower dose of kainate (10 mg/kg), which did not elicit obvious seizure activity. Even this putatively non-epileptic dose of kainate elicited marked increases in granule cell *Arc* expression in some of the mice. Notably, a significantly lower proportion of hAPP<sub>FAD</sub> mice than NTG mice had such marked *Arc* induction after receiving the lower dose of kainate (Fig. 5B). In the remainder of the mice, which showed less than maximal induction of *Arc*, the lower dose of kainate augmented *Arc* expression in granule cells only in NTG controls but not in hAPP<sub>FAD</sub> mice (Fig. 5C,D).

#### Deficits in *Arc* expression are independent of plaque deposition but influenced by $A\beta$ levels

The synaptic and behavioral deficits we identified previously in different hAPP<sub>FAD</sub> lines were independent of the deposition of  $A\beta$  as amyloid plaques (Hsia et al., 1999; Mucke et al., 2000; Palop et al., 2003). In contrast, attenuated *Arc* induction identified by quantitative RT-PCR in the entire hippocampi of another line of hAPP<sub>FAD</sub> mice was ascribed specifically to amyloid deposition (Dickey et al., 2004). However, early plaque formation in our hAPP<sub>FAD</sub> mice did not correlate with *Arc* expression in granule cells or CA1 pyramidal cells, either at baseline or after environmental exploration (Fig. 6A,B).

To further investigate whether *Arc* deficits in hAPP mice depend on plaque deposition, we compared TG mice expressing

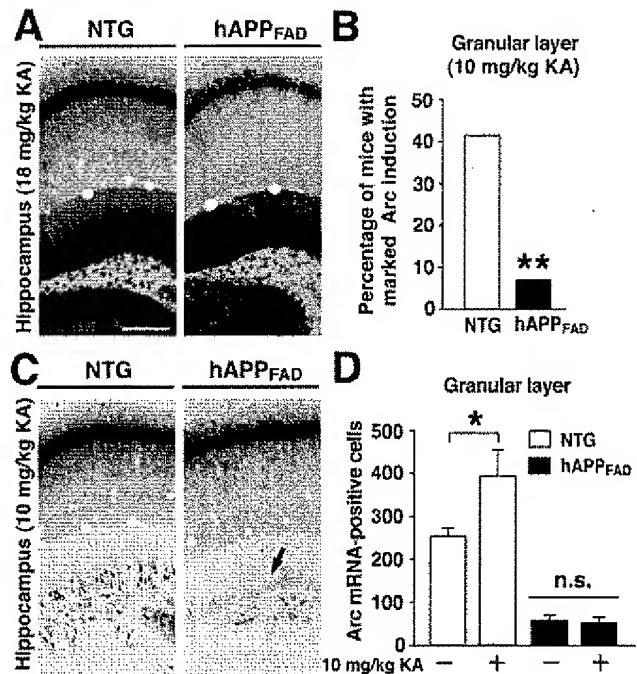


**Figure 5.** Induction of *Arc* mRNA expression by kainate. **A**, Very high levels of *Arc* mRNA in granule cells and CA1 pyramidal cells in NTG and hAPP<sub>FAD</sub> mice 2 h after injection of 18 mg/kg kainate, which elicited seizures in both groups of mice. Scale bar, 250  $\mu$ m. **B**, Proportion of mice in which injection of 10 mg/kg kainate resulted in similarly high levels of *Arc* induction in granule cells but without eliciting obvious seizure activity ( $n = 12$ –15 per genotype). \*\* $p < 0.01$  versus NTG ( $\chi^2$  test). **C, D**, In the remaining mice, 10 mg/kg kainate resulted in more moderate or no induction of *Arc* (**C**). Compared with saline-injected controls (–) of the same genotype, 10 mg/kg kainate (+) augmented *Arc* induction only in NTG controls but not in hAPP<sub>FAD</sub> mice (**C**, arrow; **D**).  $n = 4$ –5 mice per genotype for saline;  $n = 7$ –14 per genotype for kainate. \* $p < 0.05$  (Tukey–Kramer test). Error bars indicate SEM. KA, Kainate.

hAPP<sub>FAD</sub> (line J20) or hAPP<sub>WT</sub> (line I5). These lines have comparable levels of transgene expression in the brain but different levels of  $A\beta$  (Mucke et al., 2000).  $A\beta$  levels are significantly lower in line I5 than in line J20, and hAPP<sub>WT</sub> mice from line I5 never develop amyloid plaques. However, these hAPP<sub>WT</sub> mice clearly have higher  $A\beta$  levels than NTG controls and do develop subtle age-dependent synaptic deficits (Mucke et al., 2000). hAPP<sub>WT</sub> mice had less severe deficits in *Arc* and Fos expression than hAPP<sub>FAD</sub> mice (Fig. 6C,D), suggesting an  $A\beta$  dose effect that is likely independent of plaque formation. Calbindin reductions reached significance only in hAPP<sub>FAD</sub> mice, but not in hAPP<sub>WT</sub> mice (Fig. 6E), consistent with previous findings (Palop et al., 2003).

#### *Arc* expression deficits in hAPP<sub>FAD</sub> mice correlate with depletions of $\alpha$ -actinin-2 in the molecular layer

*Arc* induction critically depends on signal transduction cascades triggered by NMDA receptor activation (Lyford et al., 1995; Steward and Worley, 2001). Because the actin-binding protein  $\alpha$ -actinin-2 plays a key role in the assembly of NMDA receptors in dendritic spines as well as in the modulation of these receptors by  $Ca^{2+}$  (Wyszynski et al., 1997; Krupp et al., 1999), we examined the expression of  $\alpha$ -actinin-2 in the molecular layer of the dentate gyrus, where granule cell dendrites receive afferent input.  $\alpha$ -Actinin-2 levels were much lower in hAPP<sub>FAD</sub> mice than in NTG controls and less severely affected in hAPP<sub>WT</sub> mice (Figs. 6F and 7A). The reductions in  $\alpha$ -actinin-2 correlated tightly with deficits in *Arc* expression at baseline and after environmental exploration (Fig. 7B), suggesting that deficits in *Arc* expression

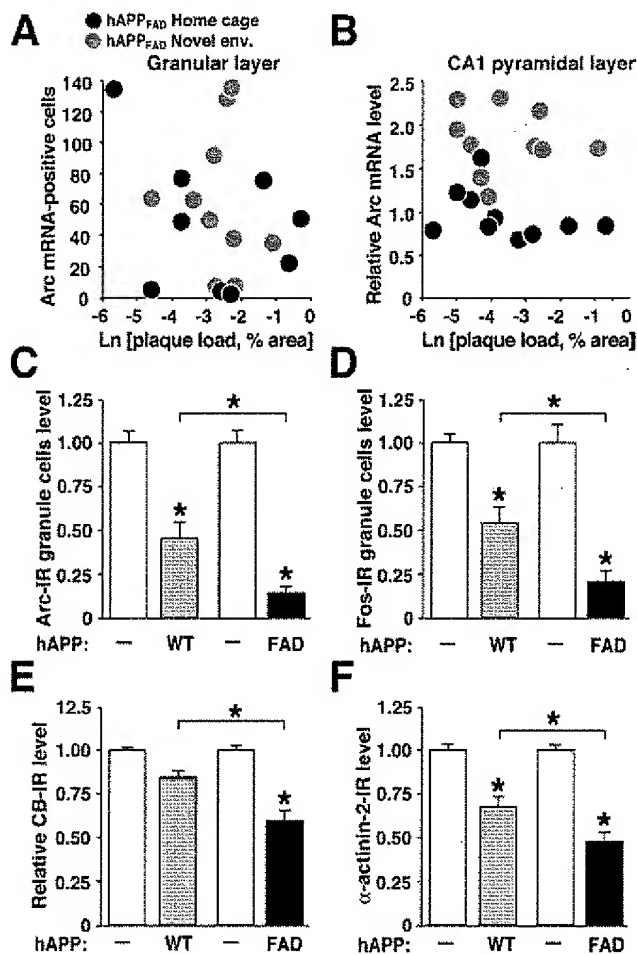


**Figure 6.** Arc expression in hAPP mice is independent of early plaque formation but influenced by the extent of Aβ production. **A, B**, Arc expression in hAPP<sub>FAD</sub> mice does not correlate with early plaque formation. Coronal brain sections of hAPP<sub>FAD</sub> mice that had (gray dots) or had not (black dots) explored a novel environment were immunostained for Aβ deposits or analyzed by *in situ* hybridization to determine the number of Arc-positive granule cells in the dentate gyrus (**A**) and relative Arc mRNA levels in the pyramidal cell layer of the CA1 region (**B**). At baseline and after exploration, neuronal Arc expression in the granular layer and in CA1 did not correlate with the extent of amyloid deposition in these regions. **C–F**, Molecular profile of granule cells in two hAPP lines with similar levels of hAPP expression but different levels of Aβ (Mucke et al., 2000). Brain sections from TG mice of hAPP<sub>WT</sub> line J5 (□) and hAPP<sub>FAD</sub> line J20 (■) and from NTG littermates of each line (□) were immunostained for Arc (**C**), Fos (**D**), calbindin (**E**), or α-actinin-2 (**F**).  $n = 9–12$  mice per group; \* $p < 0.01$  (Tukey–Kramer test). Error bars indicate SEM. Ln, Natural log.

may be related to alterations in excitatory dendritic spines. Reductions in Arc (Fig. 7C) and α-actinin-2 (data not shown) both correlated with calbindin reductions, which have been shown previously to reflect learning and memory deficits in hAPP<sub>FAD</sub> mice (Palop et al., 2003), underscoring the potential functional relevance of these molecular alterations.

#### Decreased activity of the NMDA receptor-dependent signaling pathway in the dentate gyrus of hAPP<sub>FAD</sub> mice

To assess more directly whether alterations in NMDA receptor-dependent signaling might be responsible for Arc expression deficits in hAPP<sub>FAD</sub> mice, we examined phosphorylation of tyrosine 1472 of the NR2B subunit, which increases the activity of NMDA receptors (Moon et al., 1994; Wang and Salter, 1994) and is associated with LTP induction (Rosenblum et al., 1996; Rostas et al., 1996). Western blot analysis of the dentate gyrus revealed marked

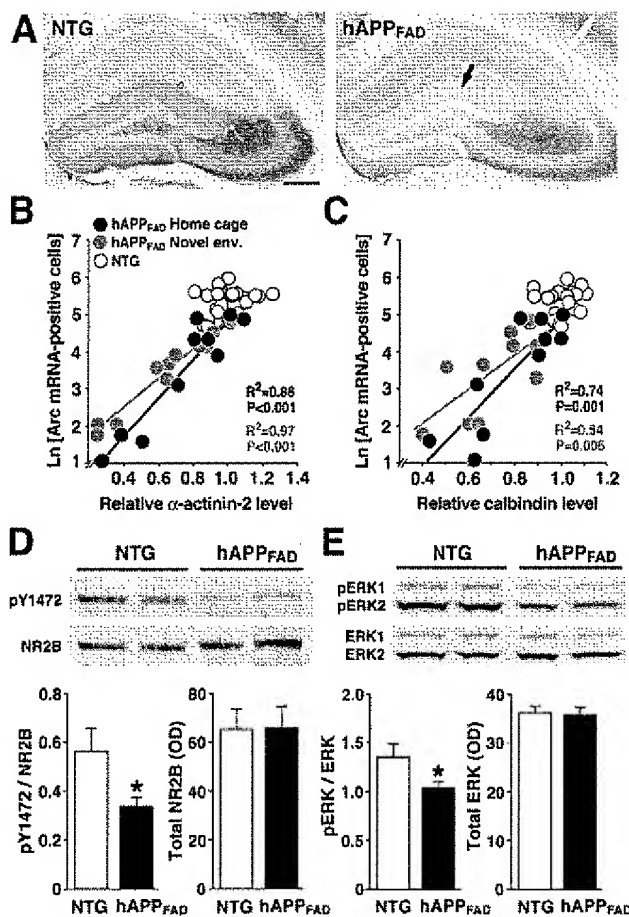


**Figure 7.** Deficits in Arc expression are associated with reductions in key components of the NMDA receptor-dependent signaling pathway. **A–C**, Arc expression deficits in granule cells of hAPP<sub>FAD</sub> mice are tightly linked to the depletion of α-actinin-2 in the molecular layer of the dentate gyrus. Coronal brain sections of NTG and hAPP<sub>FAD</sub> mice that had (gray dots) or had not (black dots) explored a novel environment were analyzed by *in situ* hybridization for Arc or immunostained for α-actinin-2 or calbindin. Representative sections in **A** illustrate robust expression of α-actinin-2 in the molecular layer of an NTG control (left) and depletion of α-actinin-2 in the molecular layer of an hAPP<sub>FAD</sub> mouse (right, arrow). Scale bar, 250 μm. At baseline and after environmental exploration, granule cell expression of Arc correlated strongly with levels of α-actinin-2 (**B**), calbindin (**C**), and Fos (data not shown) in hAPP<sub>FAD</sub> mice but not in NTG controls.  $R^2$  and  $p$  values in **B** and **C** refer to hAPP<sub>FAD</sub> mice only. Novel env., Novel environment; Ln, natural log. **D, E**, Levels of phosphorylated (activated) NR2B and ERK1/2 are reduced in the dentate gyrus of hAPP<sub>FAD</sub> mice. Western blot analysis of phosphorylated tyrosine residue 1472 of NR2B (pY1472) and total NR2B (**D**) levels and of dually phosphorylated ERK1/2 (pERK1/2) and total ERK1/2 (**E**) levels illustrates reduced levels of putatively activated NR2B and ERK1/2 in the dentate gyrus of hAPP<sub>FAD</sub> mice compared with NTG controls. Quantitation of bands on comparable blots (bottom) revealed significant reductions in the ratios of phospho/total NR2B (**D**) and in phospho/total ERK1/2 (**E**) in hAPP<sub>FAD</sub> mice compared with NTG controls and no change in the levels of total NR2B and total ERK1/2.  $n = 9–10$  mice per genotype. \* $p < 0.05$  (Student's *t* test). Error bars indicate SEM.

reductions in phosphorylated NR2B in hAPP<sub>FAD</sub> mice compared with NTG controls and no change in total NR2B levels (Fig. 7D).

Calcium influx through NMDA receptors leads to downstream phosphorylation and activation of ERK1/2, MAPK (mitogen-activated protein kinase) family members with activities that are critical for LTP (Thomas and Huganir, 2004). hAPP<sub>FAD</sub> mice had reduced levels of phosphorylated ERK1/2 in the dentate gyrus, without changes in total ERK1/2 levels (Fig. 7E). Because phosphorylation of ERK1/2 is an early event in NMDA receptor-mediated signaling, which is necessary for Arc induction (Steward and Worley, 2001), this result further sup-

ports the notion that Arc deficits in hAPP<sub>FAD</sub> mice may result from impairments in NMDA receptor-mediated signaling.

## Discussion

We used immediate-early gene expression imaging to assess the effects of hAPP/A $\beta$  on activity patterns of neuronal ensembles in the brain. Widespread neuronal expression of hAPP/A $\beta$  impaired both basal and induced expression of Arc predominantly in granule cells of the dentate gyrus. Thus, although granule cells are relatively resistant to degeneration in AD and hAPP mice (West et al., 1994; Palop et al., 2003), they are exquisitely vulnerable to hAPP/A $\beta$ -induced dysfunction. The reduced phosphorylation of NR2B and ERK1/2 in the dentate gyrus suggests that this impairment may be attributable, at least in part, to an attenuation of NMDA receptor-dependent signaling. In light of the physiological functions of Arc and the dentate gyrus (Guzowski et al., 2000; Gilbert et al., 2001), disruption of Arc expression in granule cells may contribute critically to deficits in learning and memory in hAPP mice and possibly in AD.

When entire hippocampi of hAPP/presenilin 1 doubly TG mice were analyzed by RT-PCR, basal Arc expression was found to be normal, whereas induced expression was attenuated (Dickey et al., 2004). Our results show that deficits in basal Arc levels in granule cells could easily be obscured by normal basal Arc levels in cells of other hippocampal subfields. Attenuated Arc induction in hAPP/presenilin 1 mice was ascribed specifically to amyloid deposition (Dickey et al., 2004). However, in our hAPP<sub>FAD</sub> mice, Arc expression in granule cells and CA1 pyramidal cells did not correlate with early amyloid deposition, at baseline or after stimulation. Moreover, we found qualitatively similar, albeit smaller, deficits in Arc expression in hAPP<sub>WT</sub> mice from line 15, which never develop plaques (Mucke et al., 2000). Although A $\beta$  levels are typically lower in hAPP<sub>WT</sub> mice than in transgene expression-matched hAPP<sub>FAD</sub> mice, hAPP<sub>WT</sub> mice have higher A $\beta$  levels than NTG controls and can develop age-dependent synaptic and behavioral deficits (Moechars et al., 1999; Mucke et al., 2000; Koistinaho et al., 2001). Granule cell expression of Arc and Fos in hAPP<sub>WT</sub> mice was indeed lower than in NTG mice and higher than in hAPP<sub>FAD</sub> mice, suggesting an A $\beta$  dose effect. Our findings support the notion that functional deficits in hAPP mice are more likely caused by small nonfibrillar A $\beta$  assemblies than by fibrillar A $\beta$  deposited in amyloid plaques (Hsia et al., 1999; Klein et al., 2001; Walsh and Selkoe, 2004; Cleary et al., 2005).

Independent of which particular A $\beta$  assemblies or hAPP metabolites are responsible for the molecular alterations we identified in hAPP mice, they might act both within the dentate gyrus and in regions projecting to this structure. Indeed, because Arc expression depends on excitatory synaptic activity (Lyford et al., 1995), the special vulnerability of granule cells to A $\beta$ -induced disruptions of Arc expression could be attributable to cell-autonomous effects and to alterations in network properties. Consistent with the latter possibility, the lines of hAPP mice analyzed in the current study have depletions of synaptophysin-immunoreactive presynaptic terminals in the molecular layer of the dentate gyrus (Mucke et al., 2000), where granule cells receive most of their input. It is also interesting in this regard that the Arc expression deficits in our hAPP mice resembled those in NTG rats after lesioning of the entorhinal cortex (Temple et al., 2003). The entorhinal cortex is affected early in AD (Hyman et al., 1988) and is important in computations that take place before and after cortical information enters the hippocampus (Steffenach et al., 2005). Thus, molecular alterations and synaptic impairments in

the molecular layer of the dentate gyrus in hAPP mice may reflect, at least partially, neuronal alterations in laminae II and III of the entorhinal cortex, from which granule cells receive important input.

The results of the current study suggest that A $\beta$ -induced alterations in granule cell input might trigger a vicious cycle that could progressively disable critical hippocampal functions. A decrease in NMDA receptor-dependent signaling, which is critical for the expression of Arc (Steward and Worley, 2001), may be a crucial element of this cycle. In the dentate gyrus of hAPP<sub>FAD</sub> mice, we found reductions in the phosphorylation states of the NR2B subunit, which regulates the activity of NMDA receptors (Salter and Kalia, 2004), and reductions in the MAPKs ERK1/2, the activities of which are regulated by NMDA receptors (Thomas and Huganir, 2004). In agreement with our *in vivo* results, it has been demonstrated recently in primary neuronal cultures that A $\beta$  promotes dephosphorylation of the NR2B subunit and endocytosis of NMDA receptors, attenuating NMDA-evoked currents and NMDA-dependent signaling pathways (Snyder et al., 2005).

Notably, an experimental reduction in Arc expression in the rat hippocampus impaired maintenance of LTP and consolidation of long-term memory (Guzowski et al., 2000). hAPP<sub>FAD</sub> mice from line J20 also show deficits in learning and memory that correlate tightly with depletions of calbindin and Fos in granule cells of the dentate gyrus (Palop et al., 2003), which in turn correlated with Arc deficits in the current study. Because Arc appears to participate in the modification of activated synapses as an anchoring or targeting protein (Lyford et al., 1995; Guzowski et al., 2000), its reduction could destabilize dendritic spines and contribute to reductions in other synaptic activity-dependent proteins, including Fos, calbindin, and  $\alpha$ -actinin-2, further impairing learning and memory (Molinari et al., 1996; Guzowski, 2002). Alterations in  $\alpha$ -actinin-2 and calbindin could in turn impair NMDA receptor signaling (Wyszynski et al., 1997; Krupp et al., 1999; Nägerl et al., 2000), on which Arc expression depends (Lyford et al., 1995; Steward and Worley, 2001).

Because Arc and related factors seem to be intimately involved in the encoding of specific environmental contexts (Guzowski et al., 1999; Vazdarjanova and Guzowski, 2004), the vicious cycle described above would be expected to disrupt the recruitment of granule cell ensembles during acquisition of contextual information. It is tempting to speculate that this process contributes critically to the visuospatial disabilities of hAPP mice and of patients with AD. The obliteration of encoding activity in specific neuronal populations involved in learning and memory may also contribute more generally to the impairments of declarative memory in early AD and to the inexorable loss of memory and other cognitive functions later on. The vicious cycle triggered by impairments in molecular pathways that both depend on and regulate synaptic activity might be broken not only by decreasing A $\beta$  levels in the brain but also by normalizing synaptic plasticity. These approaches are not mutually exclusive and, in combination, might provide additive or synergistic therapeutic benefits.

## References

- Braak H, Braak E (1991) Neuropathological staging of Alzheimer-related changes. *Acta Neuropathol* 82:239–259.
- Burke SN, Chawla MK, Penner MR, Crowell BE, Worley PF, Barnes CA, McNaughton BL (2005) Differential encoding of behavior and spatial context in deep and superficial layers of the neocortex. *Neuron* 45:667–674.
- Cleary JP, Walsh DM, Hofmeister JJ, Shankar GM, Kuskowski MA, Selkoe DJ, Ashe KH (2005) Natural oligomers of the amyloid- $\beta$  protein specifically disrupt cognitive function. *Nat Neurosci* 8:79–84.

- Corder EH, Woodbury MA, Volkman I, Madsen DK, Bogdanovic N, Winblad B (2000) Density profiles of Alzheimer disease regional brain pathology for the huddinge brain bank: pattern recognition emulates and expands upon Braak staging. *Exp Gerontol* 35:851–864.
- Dickey CA, Loring JF, Montgomery J, Gordon MN, Eastman PS, Morgan D (2003) Selectively reduced expression of synaptic plasticity-related genes in amyloid precursor protein + presenilin-1 transgenic mice. *J Neurosci* 23:5219–5226.
- Dickey CA, Gordon MN, Mason JE, Wilson NJ, Diamond DM, Guzowski JF, Morgan D (2004) Amyloid suppresses induction of genes critical for memory consolidation in APP + PS1 transgenic mice. *J Neurochem* 88:434–442.
- Eustache F, Piolino P, Giffard B, Viader F, De La Sayette V, Baron JC, Desgranges B (2004) "In the course of time": a PET study of the cerebral substrates of autobiographical amnesia in Alzheimer's disease. *Brain* 127:1549–1560.
- Games D, Adams D, Alessandrini R, Barbour R, Berthelette P, Blackwell C, Carr T, Clemens J, Donaldson T, Gillespie F, Guido T, Hagopian S, Johnson-Wood K, Khan K, Lee M, Leibowitz P, Lieberburg I, Little S, Masliah E, McConlogue L, et al. (1995) Alzheimer-type neuropathology in transgenic mice overexpressing V717F  $\beta$ -amyloid precursor protein. *Nature* 373:523–527.
- Gilbert PE, Kesner RP, Lee I (2001) Dissociating hippocampal subregions: A double dissociation between dentate gyrus and CA1. *Hippocampus* 11:626–636.
- Guzowski JF (2002) Insights into immediate-early gene function in hippocampal memory consolidation using antisense oligonucleotide and fluorescent imaging approaches. *Hippocampus* 12:86–104.
- Guzowski JF, McNaughton BL, Barnes CA, Worley PF (1999) Environment-specific expression of the immediate-early gene *Arc* in hippocampal neuronal ensembles. *Nat Neurosci* 2:1120–1124.
- Guzowski JF, Lyford GL, Stevenson GD, Houston FP, McGaugh JL, Worley PF, Barnes CA (2000) Inhibition of activity-dependent *arc* protein expression in the rat hippocampus impairs the maintenance of long-term potentiation and the consolidation of long-term memory. *J Neurosci* 20:3993–4001.
- Higgins GA, Jacobsen H (2003) Transgenic mouse models of Alzheimer's disease: phenotype and application. *Behav Pharmacol* 14:419–438.
- Hsia A, Masliah E, McConlogue L, Yu G, Tatsuno G, Hu K, Kholodenko D, Malenka RC, Nicoll RA, Mucke L (1999) Plaque-independent disruption of neural circuits in Alzheimer's disease mouse models. *Proc Natl Acad Sci USA* 96:3228–3233.
- Hyman BT, Kromer LJ, Van Hoesen GW (1988) A direct demonstration of the perforant pathway terminal zone in Alzheimer's disease using the monoclonal antibody Alz-50. *Brain Res* 450:392–397.
- Klein WL, Krafft GA, Finch CE (2001) Targeting small  $A\beta$  oligomers: the solution to an Alzheimer's disease conundrum. *Trends Neurosci* 24:219–224.
- Kobayashi DT, Chen KS (2005) Behavioral phenotypes of amyloid-based genetically modified mouse models of Alzheimer's disease. *Genes Brain Behav* 4:173–196.
- Koistinaho M, Ort M, Cimadevilla JM, Vondrouk R, Cordell B, Koistinaho J, Bures J, Higgins LS (2001) Specific spatial learning deficits become severe with age in  $\beta$ -amyloid precursor protein transgenic mice that harbor diffuse  $\beta$ -amyloid deposits but do not form plaques. *Proc Natl Acad Sci USA* 98:14675–14680.
- Krupp JJ, Vissel B, Thomas CG, Heinemann SF, Westbrook GL (1999) Interactions of calmodulin and  $\alpha$ -actinin with the NR1 subunit modulate  $Ca^{2+}$ -dependent inactivation of NMDA receptors. *J Neurosci* 19:1165–1178.
- Lyford GL, Yamagata K, Kaufmann WE, Barnes CA, Sanders LK, Copeland NG, Gilbert DJ, Jenkins NA, Lanahan AA, Worley PF (1995) *Arc*, a growth factor and activity-regulated gene, encodes a novel cytoskeleton-associated protein that is enriched in neuronal dendrites. *Neuron* 14:433–445.
- Moechars D, Dewachter I, Lorent K, Reverse D, Backelant V, Naidu A, Teseur J, Spittaels K, Van Den Haute C, Checler F, Godaux E, Cordell B, Van Leuven F (1999) Early phenotypic changes in transgenic mice that overexpress different mutants of amyloid precursor protein in brain. *J Biol Chem* 274:6483–6492.
- Molinari S, Battini R, Ferrari S, Pozzi L, Killcross AS, Robbins TW, Jouvenceau A, Billard J-M, Dutar P, Lamour Y, Baker WA, Cox H, Emson PC (1996) Deficits in memory and hippocampal long-term potentiation in mice with reduced calbindin  $D_{28K}$  expression. *Proc Natl Acad Sci USA* 93:8028–8033.
- Moon IS, Apperson ML, Kennedy MB (1994) The major tyrosine-phosphorylated protein in the postsynaptic density fraction is N-methyl-D-aspartate receptor subunit 2B. *Proc Natl Acad Sci USA* 91:3954–3958.
- Mucke L, Masliah E, Yu G-Q, Mallory M, Rockenstein EM, Tatsuno G, Hu K, Kholodenko D, Johnson-Wood K, McConlogue L (2000) High-level neuronal expression of  $A\beta_{1-42}$  in wild-type human amyloid protein precursor transgenic mice: synaptotoxicity without plaque formation. *J Neurosci* 20:4050–4058.
- Nägerl UV, Mody I, Jeub M, Lie AA, Elger CE, Beck H (2000) Surviving granule cells of the sclerotic human hippocampus have reduced  $Ca^{2+}$  influx because of a loss of calbindin- $D_{28K}$  in temporal lobe epilepsy. *J Neurosci* 20:1831–1836.
- Palop JJ, Jones B, Kekonius L, Chin J, Yu G-Q, Raber J, Masliah E, Mucke L (2003) Neuronal depletion of calcium-dependent proteins in the dentate gyrus is tightly linked to Alzheimer's disease-related cognitive deficits. *Proc Natl Acad Sci USA* 100:9572–9577.
- Rockenstein EM, McConlogue L, Tan H, Gordon M, Power M, Masliah E, Mucke L (1995) Levels and alternative splicing of amyloid  $\beta$  protein precursor (APP) transcripts in brains of transgenic mice and humans with Alzheimer's disease. *J Biol Chem* 270:28257–28267.
- Rosenblum K, Dudai Y, Richter-Levin G (1996) Long-term potentiation increases tyrosine phosphorylation of the N-methyl-D-aspartate receptor subunit 2B in rat dentate gyrus *in vivo*. *Proc Natl Acad Sci USA* 93:10457–10460.
- Rostas JA, Brent VA, Voss K, Errington ML, Bliss TV, Gurd JW (1996) Enhanced tyrosine phosphorylation of the 2B subunit of the N-methyl-D-aspartate receptor in long-term potentiation. *Proc Natl Acad Sci USA* 93:10452–10456.
- Sadek JR, Johnson SA, White DA, Salmon DP, Taylor KI, Delapena JH, Paulsen JS, Heaton RK, Grant I (2004) Retrograde amnesia in dementia: comparison of HIV-associated dementia, Alzheimer's disease, and Huntington's disease. *Neuropsychology* 18:692–699.
- Salter MW, Kalia LV (2004) Src kinases: a hub for NMDA receptor regulation. *Nat Rev Neurosci* 5:317–328.
- Snyder EM, Nong Y, Almeida CG, Paul S, Moran T, Choi EY, Nairn AC, Salter MW, Lombroso PJ, Goursa GK, Greengard P (2005) Regulation of NMDA receptor trafficking by amyloid- $\beta$ . *Nat Neurosci* 8:1051–1058.
- Steffenach HA, Witter M, Moser MB, Moser EI (2005) Spatial memory in the rat requires the dorsolateral band of the entorhinal cortex. *Neuron* 45:301–313.
- Steward O, Worley PF (2001) Selective targeting of newly synthesized *Arc* mRNA to active synapses requires NMDA receptor activation. *Neuron* 30:227–240.
- Temple MD, Worley PF, Steward O (2003) Visualizing changes in circuit activity resulting from denervation and reinnervation using immediate early gene expression. *J Neurosci* 23:2779–2788.
- Thomas GM, Hagan RL (2004) MAPK cascade signalling and synaptic plasticity. *Nat Rev Neurosci* 5:173–183.
- Vazdarjanova A, Guzowski JF (2004) Differences in hippocampal neuronal population responses to modifications of an environmental context: evidence for distinct, yet complementary, functions of CA3 and CA1 ensembles. *J Neurosci* 24:6489–6496.
- Walsh DM, Selkoe DJ (2004) Deciphering the molecular basis of memory failure in Alzheimer's disease. *Neuron* 44:181–193.
- Wang YT, Salter MW (1994) Regulation of NMDA receptors by tyrosine kinases and phosphatases. *Nature* 369:233–235.
- West MJ, Slomianka L, Gundersen HJG (1991) Unbiased stereological estimation of the total number of neurons in the subdivisions of the rat hippocampus using the optical fractionator. *Anat Rec* 231:482–497.
- West MJ, Coleman PD, Flood DG, Troncoso JC (1994) Differences in the pattern of hippocampal neuronal loss in normal ageing and Alzheimer's disease. *Lancet* 344:769–772.
- Wiltgen BJ, Brown RA, Talton LE, Silva AJ (2004) New circuits for old memories: the role of the neocortex in consolidation. *Neuron* 44:101–108.
- Wyszynski M, Lin J, Rao A, Nigh E, Beggs AH, Craig AM, Sheng M (1997) Competitive binding of  $\alpha$ -actinin and calmodulin to the NMDA receptor. *Nature* 385:439–442.

# Fyn Kinase Induces Synaptic and Cognitive Impairments in a Transgenic Mouse Model of Alzheimer's Disease

Jeannie Chin,<sup>1,2</sup> Jorge J. Palop,<sup>1,2</sup> Jukka Puolivali,<sup>1,2</sup> Catherine Massaro,<sup>1,3</sup> Nga Bien-Ly,<sup>1</sup> Hilary Gerstein,<sup>1</sup> Kimberly Searce-Levie,<sup>1</sup> Eliezer Masliah,<sup>4</sup> and Lennart Mucke<sup>1,2,3</sup>

<sup>1</sup>Gladstone Institute of Neurological Disease, <sup>2</sup>Department of Neurology, and <sup>3</sup>Neuroscience Graduate Program, University of California, San Francisco, San Francisco, California 94158, and <sup>4</sup>Departments of Neurosciences and Pathology, University of California at San Diego, La Jolla, California 92093

Human amyloid precursor protein (hAPP) transgenic mice with high levels of amyloid- $\beta$  ( $A\beta$ ) develop behavioral deficits that correlate with the depletion of synaptic activity-related proteins in the dentate gyrus. The tyrosine kinase Fyn is altered in Alzheimer's disease brains and modulates premature mortality and synaptotoxicity in hAPP mice. To determine whether Fyn also modulates  $A\beta$ -induced behavioral deficits and depletions of synaptic activity-dependent proteins, we overexpressed Fyn in neurons of hAPP mice with moderate levels of  $A\beta$  production. Compared with nontransgenic controls and singly transgenic mice expressing hAPP or FYN alone, doubly transgenic FYN/hAPP mice had striking depletions of calbindin, Fos, and phosphorylated ERK (extracellular signal-regulated kinase), impaired neuronal induction of Arc, and impaired spatial memory retention. These deficits were qualitatively and quantitatively similar to those otherwise seen only in hAPP mice with higher  $A\beta$  levels. Surprisingly, levels of active Fyn were lower in high expresser hAPP mice than in NTG controls and lower in FYN/hAPP mice than in FYN mice. Suppression of Fyn activity may result from dephosphorylation by striatal-enriched phosphatase, which was upregulated in FYN/hAPP mice and in hAPP mice with high levels of  $A\beta$ . Thus, increased Fyn expression is sufficient to trigger prominent neuronal deficits in the context of even relatively moderate  $A\beta$  levels, and inhibition of Fyn activity may help counteract  $A\beta$ -induced impairments.

**Key words:** hippocampus; plasticity; amyloid  $\beta$ ; Arc; spatial memory; striatal-enriched phosphatase (STEP)

## Introduction

The amyloid precursor protein (APP) is expressed at high levels in synapses in which it appears to play roles in synaptic plasticity and neurite outgrowth (Turner et al., 2003). APP undergoes proteolytic cleavage resulting in several metabolites, including amyloid- $\beta$  ( $A\beta$ ) peptides (Turner et al., 2003). Abnormal accumulation and deposition of  $A\beta$  are pathological hallmarks of Alzheimer's disease (AD), which is associated with progressive cognitive decline and degeneration of synapses and neurons. However, the precise relationship between  $A\beta$ , synaptic impairments, and cognitive decline remains uncertain (Walsh and Selkoe, 2004).

APP/ $A\beta$ -induced neuronal and behavioral deficits have been investigated in several transgenic (TG) mouse models (Higgins and Jacobsen, 2003; Gotz et al., 2004; Kobayashi and Chen, 2005). Findings from many of these models, as well as from *in vitro* studies, are consistent with the hypothesis that small nonfibrillar assemblies of  $A\beta$  can aberrantly engage intracellular signaling

pathways in neurons and thereby disrupt normal synaptic function (Lambert et al., 1998; Hsia et al., 1999; Klein et al., 2001; Verdier and Penke, 2004; Walsh and Selkoe, 2004). Several cell-surface receptors have been identified that might mediate these  $A\beta$  effects, including integrins (Sabo et al., 1995; Bi et al., 2002; Grace et al., 2002), nicotinic acetylcholine receptors (nAChRs) (Dineley et al., 2001), the p75 neurotrophin receptor (Yaar et al., 1997), and the receptor for advanced glycation end products (Yan et al., 1996; Arancio et al., 2004). Many of these receptors are located at the postsynaptic membrane, providing  $A\beta$  with a suitable vantage point from which to disrupt synaptic function.

Several signaling molecules that transduce receptor-activated signals are localized beneath the postsynaptic membrane and modulate cell–cell adhesion, receptor clustering, or the scaffolding of signaling molecules (Kennedy, 1997). One of these molecules is Fyn, a member of the Src family of tyrosine kinases (Thomas and Brugge, 1997). Strategically located at the postsynaptic density of glutamatergic synapses, it is in an excellent position to modulate the effects of  $A\beta$  on synapses. Indeed, Fyn activation occurs during engagement of integrins and glutamate receptors (Roskoski, 2004; Salter and Kalia, 2004), both of which have been implicated in  $A\beta$ -induced disruption of synaptic function (Klein et al., 2001; Grace et al., 2002; Williamson et al., 2002). Furthermore, the distribution and levels of Fyn are altered in AD brains (Shirazi and Wood, 1993; Ho et al., 2004), and the toxic effects of  $A\beta$ -derived diffusible ligands on murine hippocampal slices were blocked by the genetic ablation of Fyn (Lambert et al.,

Received July 19, 2005; revised Aug. 30, 2005; accepted Sept. 3, 2005.

This work was supported by fellowships from the John Douglas French Alzheimer's Foundation (J.C.) and the Academy of Finland (J.P.) and by National Institutes of Health Grants NS41787 and AG022074 (L.M.). We thank N. Kojima for Fyn transgenic mice; P. Worley for the anti-Arc antibody; G.-Q. Yu, X. Wang, and H. Ordoñez for technical assistance; and D. Murray McPherson for administrative assistance.

Correspondence should be addressed to Dr. Lennart Mucke, Gladstone Institute of Neurological Disease, 1650 Owens Street, San Francisco, CA 94158. E-mail: lmucke@gladstone.ucsf.edu.

J. Puolivali's present address: Cerebrion Ltd., Mikrokatu 1, P.O. Box 1788, 70211 Kuopio, Finland.

DOI:10.1523/JNEUROSCI.2980-05.2005

Copyright © 2005 Society for Neuroscience 0270-6474/05/259694-10\$15.00/0



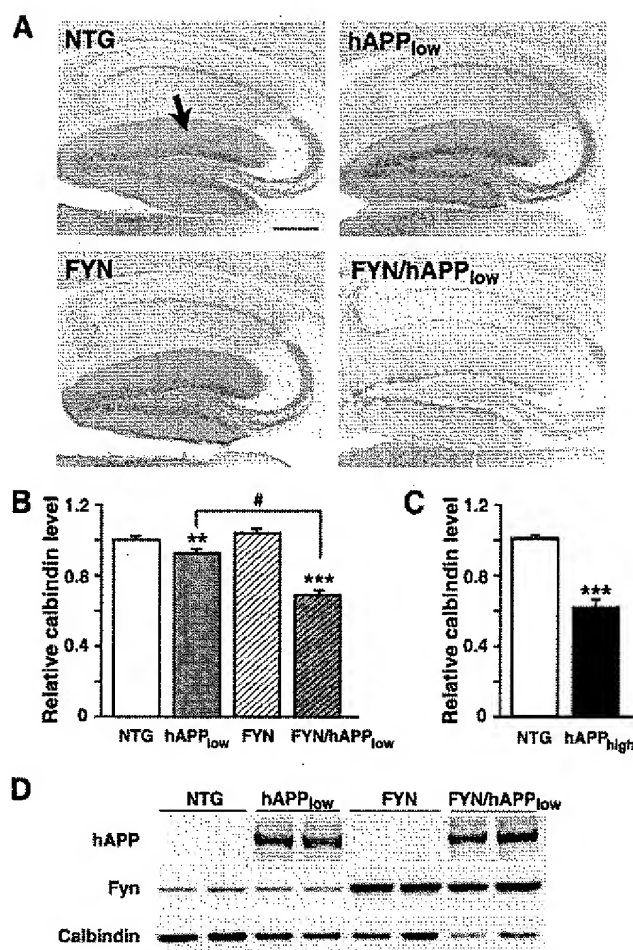


**Figure 1.** Increased expression of Fyn triggers hAPP/A $\beta$ -induced depletion of calbindin in the dentate gyrus. *A*, Immunostaining for calbindin in the molecular layer of the dentate gyrus (arrow) demonstrates marked depletion in a severely affected FYN/hAPP<sup>low</sup> mouse compared with NTG and singly TG mice. *B*, *C*, Quantitation of relative calbindin immunoreactivity (IR) levels in the molecular layer of the dentate gyrus in 23–37 mice per genotype (*B*) and 9 mice per genotype (*C*). The interaction between hAPP<sup>low</sup> and FYN was significant by ANOVA ( $p < 0.001$ ). \*\* $p < 0.01$ , \*\*\* $p < 0.001$  versus NTG; # $p < 0.05$ . *D*, Western blot analysis of dentate gyrus lysates demonstrates comparable levels of hAPP (top) and Fyn (middle) overexpression in singly TG and FYN/hAPP<sup>low</sup> mice, as well as calbindin reductions in FYN/hAPP<sup>low</sup> mice (bottom). Scale bar, 250  $\mu$ m.

1998). Finally, ablation of Fyn decreased, whereas overexpression of Fyn increased, A $\beta$ -induced synaptotoxicity and premature mortality in human APP (hAPP) mice (Chin et al., 2004). Together, these results suggest that A $\beta$  may derange synaptic functions by aberrantly engaging Fyn-related signaling pathways.

Here, we tested the hypothesis that increased neuronal activity of Fyn can trigger and exacerbate A $\beta$ -induced neuronal and behavioral deficits. Increasing Fyn activity in neurons elicited memory impairments in TG mice with moderate levels of hAPP/A $\beta$  expression and significantly exacerbated their depletion of synaptic activity-related proteins, creating a striking phenocopy of functional and molecular impairments typically seen only in mice with much higher levels of A $\beta$ . These results highlight the potential significance of pathogenic interactions between hAPP/A $\beta$  and Fyn-related signaling pathways.

## Materials and Methods

**TG mice.** hAPP TG lines J9 and J20 produce hAPP carrying the Swedish (K670N, M671L) and Indiana (V717F) familial AD mutations (hAPP770

numbering) directed by the platelet-derived growth factor (PDGF)  $\beta$  chain promoter (Rockenstein et al., 1995; Mucke et al., 2000). The lines were crossed for >10 generations onto a C57BL/6 background using NTG mice from The Jackson Laboratory (Bar Harbor, ME). Heterozygous FYN TG mice (line N8) overexpress wild-type mouse Fyn directed by the calcium/calmodulin-dependent protein kinase II $\alpha$  promoter on a C57BL/6 background (Kojima et al., 1997, 1998). Unless indicated otherwise, mice were evaluated at 6–8 months of age. To decrease variability, only male mice were assessed in the Morris water maze; all other measurements were performed on gender-balanced groups. Mice were anesthetized and flush-perfused transcardially with PBS. Hemibrains were fixed in 4% phosphate-buffered paraformaldehyde or stored at  $-70^{\circ}\text{C}$ . All experiments were approved by the Committee on Animal Research of the University of California, San Francisco.

**Immunohistochemistry.** Sliding microtome sections (30  $\mu$ m) were avidin–biotin/immunoperoxidase stained using the following primary antibodies: anti-calbindin (1:15,000; rabbit polyclonal; Swant, Bellinzona, Switzerland), anti-Fos (1:10,000; rabbit polyclonal Ab-5; Oncogene, San Diego, CA), anti-dually phosphorylated extracellular signal-regulated kinase 1/2 (phospho-ERK1/2; 1:100; rabbit polyclonal; Cell Signaling, Beverly, MA), anti-Arc (1:8000; rabbit polyclonal; a gift from Dr. P. Worley, Johns Hopkins University, Baltimore, MD), and biotinylated anti-A $\beta$  (1:500; mouse monoclonal 3D6; Elan Pharmaceuticals, South San Francisco, CA). Biotinylated goat anti-rabbit (1:200; Vector Laboratories, Burlingame, CA) was used as the secondary antibody. Diaminobenzidine was used as a chromogen. For the analysis of calbindin-immunoreactive (IR) structures, two coronal sections (300  $\mu$ m apart) per mouse between  $-2.54$  and  $-2.80$  mm from bregma were selected. The integrated optical density (IOD) of immunostains was determined with BioQuant Image Analysis (R&M Biometrics, Nashville, TN) and averaged in two areas (0.04 mm<sup>2</sup> each) of the molecular layer of the dentate gyrus and of the stratum radiatum of the CA1 region. Relative calbindin-IR levels were expressed as the ratio of IODs in the molecular layer and in the stratum radiatum of the same section. The mean ratio of nontransgenic (NTG) mice was defined as 1. The relative numbers of Fos-IR, phospho-ERK1/2-IR, and Arc-IR granule cells were determined by counting labeled cells in the granular layer in every 10th serial coronal section throughout the rostro-caudal extent of the granular layer. For plaque-load determination, the average percentage area of the hippocampus occupied by A $\beta$ -IR deposits was determined in four coronal sections (300  $\mu$ m apart) per mouse, as described previously (Mucke et al., 2000).

Vibratome sections (50  $\mu$ m) were labeled with anti-glial fibrillary acidic protein (GFAP; 1:500; Chemicon, Temecula, CA) as described previously (Togias et al., 1994; Mucke et al., 1995), followed by a biotinylated species-specific secondary IgG (1:200; Vector Laboratories). After development with diaminobenzidine, relative levels of immunoreactivity were determined densitometrically with a Quantimet 570C (Leica, Arcadia, CA).

**Immunoprecipitation and Western blot analysis.** A McIlwain tissue chopper was used to cut hemibrains into 450- $\mu$ m-thick horizontal sections from which the dentate gyrus was microdissected on ice. For protein quantitations, dentate gyrus samples from each hemibrain were pooled and homogenized on ice in buffer containing 320 mM sucrose, 10 mM Tris-HCl, pH 7.4, 10 mM EDTA, 10 mM EGTA, 1% deoxycholate, 1 mM PMSF, Phosphatase Inhibitor Cocktails I and II (Sigma), and protease inhibitor mixture (Roche). Samples were then briefly sonicated on ice and centrifuged at 5000  $\times$  g for 10 min. Equal amounts of protein (determined by the Bradford assay) were resolved by SDS-PAGE on 4–12% gradient gels and transferred to nitrocellulose membranes. For immunoprecipitations, 70  $\mu$ g of protein were incubated overnight at 4 $^{\circ}\text{C}$  with 5  $\mu$ l of goat-anti-Fyn polyclonal antibody (Santa Cruz Biotechnology, Santa Cruz, CA). Protein G-coupled magnetic beads were then added to precipitate antibody-bound proteins. After washing the beads, 2 $\times$  sample buffer was added to liberate the antibody–protein complexes, and samples were resolved by SDS-PAGE. For analysis of phosphoproteins, membranes were labeled with anti-Tyr<sup>416</sup>, which recognizes active Fyn (1:1000; rabbit polyclonal; Cell Signaling), followed by incubation with HRP-conjugated goat anti-rabbit IgG (1:5000; Chemicon) secondary antibody. For analysis of total Fyn levels, blots were stripped

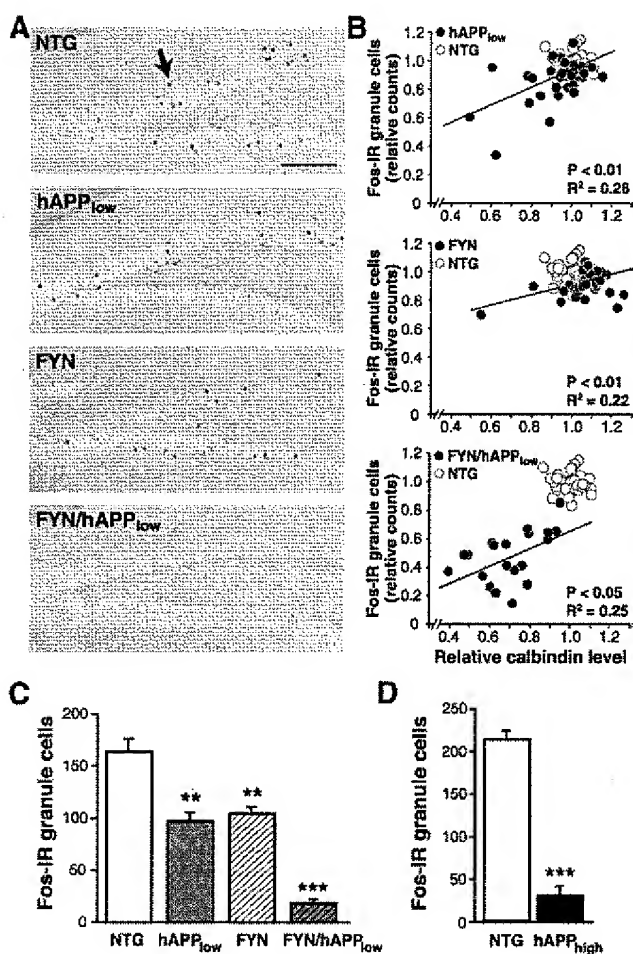


**Figure 2.** hAPP/A $\beta$  and Fyn cooperate to diminish the number of Fos-positive granule cells in FYN/hAPP<sub>low</sub> mice. *A*, Immunostaining for Fos demonstrates a typical pattern of granule cell labeling (arrow) in the dentate gyrus of an NTG mouse and different degrees of Fos reduction in TG mice. FYN/hAPP<sub>low</sub> mice were affected most severely. *B*, Calbindin levels correlated with the number of Fos-positive granule cells in singly and doubly TG mice but not in NTG controls. The  $p$  and  $R^2$  values refer to TG groups only. *C*, *D*, Quantitation of Fos-positive granule cells revealed significant reductions in hAPP<sub>low</sub> and FYN mice (*C*). FYN/hAPP<sub>low</sub> mice had more severe depletions (*C*) that were of similar magnitude as those in hAPP<sub>high</sub> mice (*D*).  $n = 23$ –37 (*C*) or  $n = 9$  (*D*) mice per genotype. \*\* $p < 0.01$ , \*\*\* $p < 0.001$  versus NTG. Scale bar, 100  $\mu$ m.

and reprobbed with anti-Fyn (1:1000; mouse monoclonal; BD Transduction Laboratories, San Jose, CA). The following antibodies were used for Western blot analyses and detected with species-appropriate HRP-conjugated secondary antibodies: anti-human APP (1:1000; Elan Pharmaceuticals), anti-striatal-enriched phosphatase (STEP; 1:5000; mouse monoclonal; Novus Biologicals, Littleton, CO), anti- $\alpha 7$  nAChR (1:1000; mouse monoclonal; Covance, Princeton, NJ), and anti-calbindin (1:15,000; rabbit polyclonal; Swant). Bands were visualized by ECL and quantitated densitometrically with Quantity One 4.0 software (Bio-Rad, Hercules, CA).

**Novel environment.** Mice were singly housed for 3 d before the experiment. Mice assigned to novel environment exploration were transferred to an adjacent room that was different in size, shape, light, and furnishing and placed into another cage. The new cage was kept uncovered and contained a different type of bedding as well as five novel objects. The mice were allowed to explore the new environment for 2 h, whereas the remaining mice were kept undisturbed in their home cages.

The activity of the mice and their interactions with the novel objects were quantified from video records during the first 10 min of each hour the mice spent in the new cage. Activities included ambulatory movements, rearing, sniffing, and digging. Overall activity was counted as the

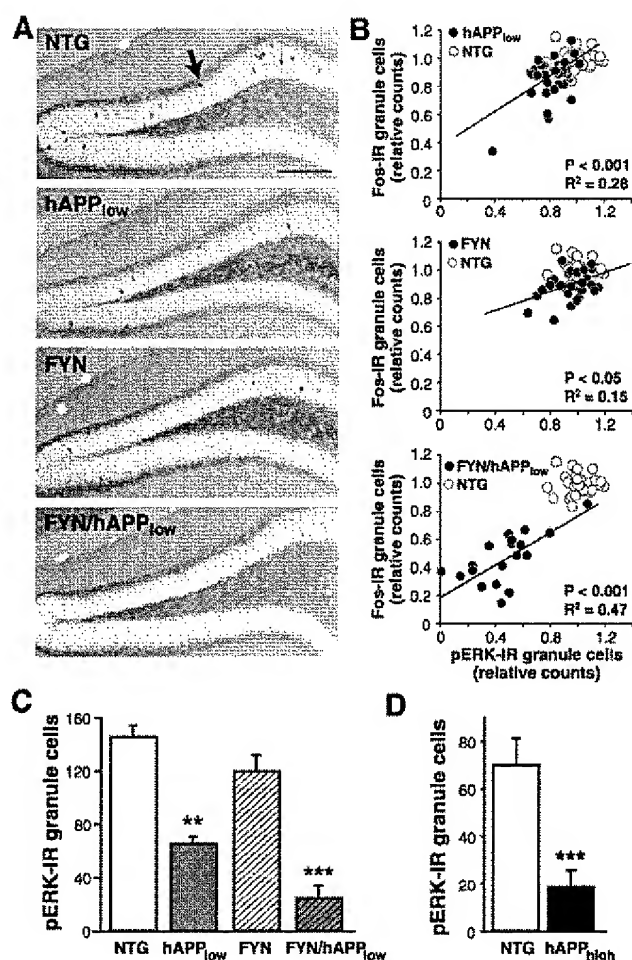


**Figure 3.** hAPP/A $\beta$  and Fyn cooperate to diminish the number of pERK1/2-positive granule cells in FYN/hAPP<sub>low</sub> mice. *A*, Immunostaining for phosphorylated ERK1/2 (pERK1/2) demonstrates a typical pattern of granule cell labeling (arrow) in the dentate gyrus of an NTG mouse and different degrees of pERK1/2 reduction in TG mice. FYN/hAPP<sub>low</sub> mice were affected most severely. *B*, Significant correlations between the numbers of pERK1/2- and Fos-positive granule cells were identified in singly and doubly TG mice but not in NTG controls. The  $p$  and  $R^2$  values refer to TG groups only. *C*, *D*, Quantitation of pERK1/2-positive granule cells revealed a significant reduction in hAPP<sub>low</sub> mice (*C*). FYN/hAPP<sub>low</sub> mice had more severe depletions (*C*) that were of similar magnitude as those in hAPP<sub>high</sub> mice (*D*).  $n = 23$ –37 (*C*) or  $n = 9$  (*D*) mice per genotype. \*\* $p < 0.01$ , \*\*\* $p < 0.001$  versus NTG. Scale bar, 100  $\mu$ m.

proportion of time the mice were engaged in any of these behaviors. An object interaction event was defined as any type of close exploratory activity with any of the five novel objects. Observers were blinded with respect to the genotype of mice.

At the end of the observation period, alternate mice assigned to the home cage or novel environment condition were taken to another room, deeply anesthetized, and perfused transcardially.

**Morris water maze.** The water maze pool (diameter, 122 cm) contained opaque water (22–23°C) with a platform (diameter, 10 cm) submerged 1.5 cm. A black and white striped mast (15 cm in height) was mounted on the platform for cued training sessions and removed for hidden platform sessions. For hidden platform sessions, the platform (14 × 14 cm) was submerged 1.5 cm and was not cued. Mice were trained to locate the cued platform (sessions 1–6) and the hidden platform (sessions 7–16) in two daily sessions (3.5 h apart), each consisting of two 60 s trials (cued training) or three 60 s trials (hidden training) with a 15 min intertrial interval. The platform location was changed for each cued platform session but remained constant in the hidden platform sessions. Entry points were changed semirandomly between trials. Twenty-four hours after completion of the hidden platform training, a 60 s probe trial (platform re-



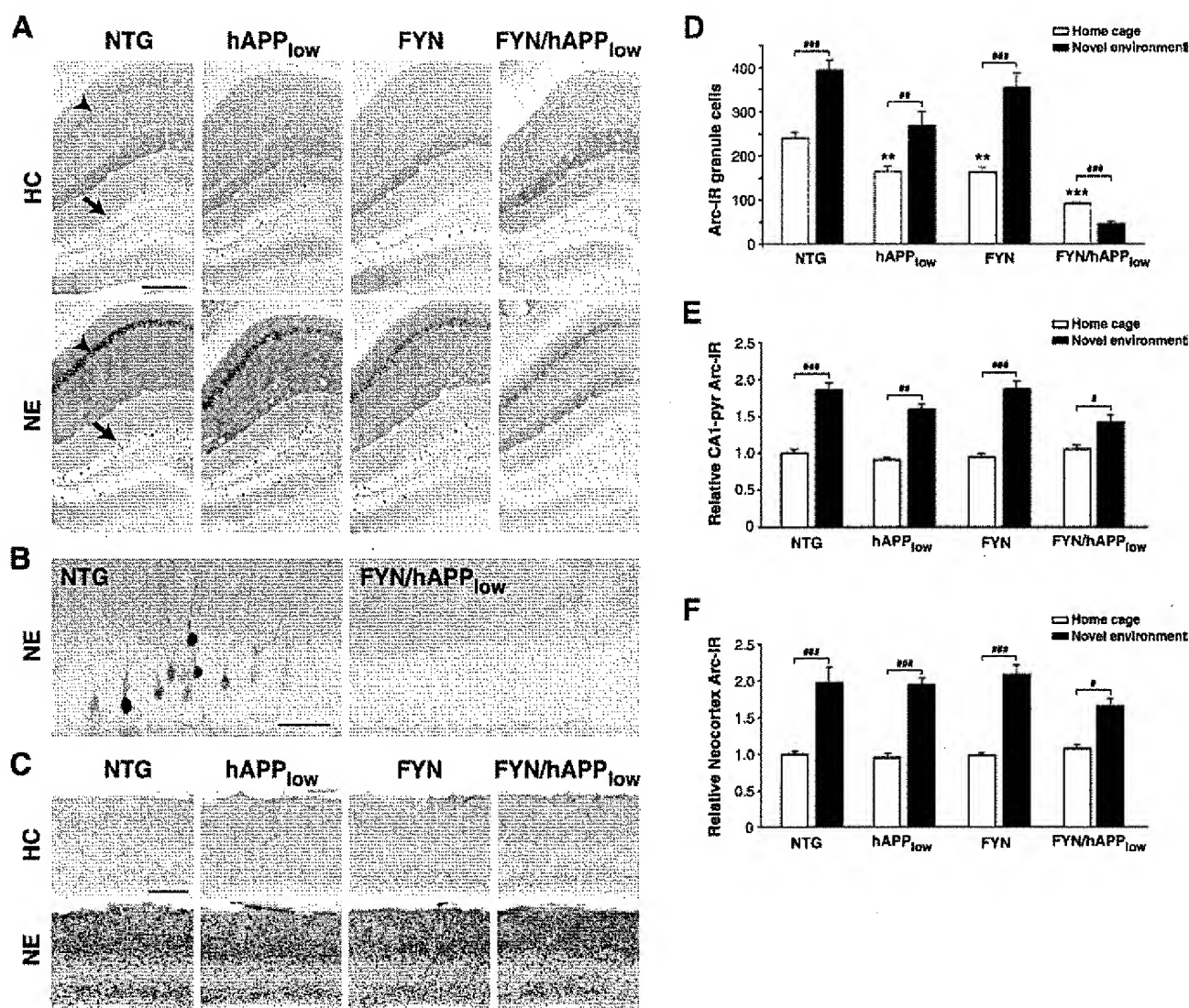


**Figure 4.** Impaired induction of Arc expression in FYN/hAPP<sub>low</sub> mice. **A**, Micrographs demonstrating Arc-IR granule cells in the dentate gyrus (arrow) and pyramidal cells in CA1 (arrowhead) in home-caged mice (HC; top) and mice that had explored a novel environment (NE; bottom). **B**, High-magnification micrographs illustrating that granule cells in the dentate gyrus were Arc immunoreactive in an NTG mouse (left), but not in a FYN/hAPP<sub>low</sub> mouse (right), after exploration of a novel environment. **C**, Micrographs demonstrating Arc-IR cells in the neocortex of mice that had (bottom) or had not (top) explored the novel environment. **D–F**, Quantitation of Arc immunolabeling ( $n = 3–10$  mice per genotype and condition) demonstrates that environmental exploration increased the number of Arc-positive granule cells in NTG and singly TG mice but not in FYN/hAPP<sub>low</sub> mice (**D**). In contrast, environmental exploration increased Arc induction in the pyramidal (Pyr) cell layer of the CA1 region (**E**) and the neocortex (**F**) also in FYN/hAPP<sub>low</sub> mice, although to a somewhat lesser extent than in NTG and FYN mice. For CA1 and neocortex data, measurements in each bar were normalized against the mean of the home-caged NTG mice. \*\* $p < 0.01$ , \*\*\* $p < 0.001$  versus NTG by ANOVA; \* $p < 0.01$ , \*\*\* $p < 0.001$  by Fisher's PLSD *post hoc* test. Scale bars: **A**, **C**, 250  $\mu\text{m}$ ; **B**, 50  $\mu\text{m}$ .

moved) was performed. Entry points for probe trials were in the west quadrant, and the target quadrant was the southeast quadrant. Performance was monitored with an EthoVision video-tracking system (Noldus Information Technology, Wageningen, The Netherlands).

**Elevated plus maze.** The elevated plus-shaped maze consisted of two open arms and two closed arms equipped with rows of infrared photocells interfaced with a computer (Hamilton, Poway, CA) as described previously (Raber et al., 2000). Briefly, mice were placed individually into the center of the maze and allowed to explore the apparatus for 10 min. The number of beam breaks was recorded to calculate the amount of time spent and distance moved in each arm, as well as the number of times the mice extended over the edges of the open arms. The apparatus was cleaned with 0.25% bleach between the testing of each mouse to standardize odors.

**Statistical analyses.** Statistical analyses were performed with Statview 5.0 (SAS Institute, Cary, NC) or SPSS-10 (SPSS, Chicago, IL). Differences between means were assessed by Student's *t* test, Mann–Whitney *U* test,

one-factor ANOVA, or two-factor ANOVA, followed by Tukey–Kramer or Fisher's PLSD *post hoc* tests. Correlations were assessed by simple regression analysis. The numbers of IR cells analyzed in the regressions are shown as relative values (compared with the mean of NTG mice) of the natural log of the total numbers of IR cells counted in each mouse.

## Results

To test for copathogenic effects between hAPP/A $\beta$  and Fyn, we crossed heterozygous TG mice from a PDGF-hAPP line with moderate levels of neuronal hAPP/A $\beta$  expression (J9, “hAPP<sub>low</sub>”) (Hsia et al., 1999; Mucke et al., 2000; Chin et al., 2004) with heterozygous TG mice from a CamKII $\alpha$ -FYN line (line N8) with increased neuronal levels of wild-type mouse Fyn (Kojima et al., 1997, 1998). The cross yielded four genotypes: NTG mice, singly TG hAPP mice, singly TG FYN mice, and doubly TG FYN/hAPP mice. These groups of mice were com-

pared with heterozygous TG mice from a PDGF-hAPP line with higher levels of neuronal hAPP/A $\beta$  expression (J20, "hAPP<sub>high</sub>") (Mucke et al., 2000; Palop et al., 2003; Chin et al., 2004).

#### Increased expression of Fyn exacerbates hAPP/A $\beta$ -induced depletion of calbindin and Fos

The calcium-binding protein calbindin-D<sub>28k</sub> regulates intracellular calcium levels and is important for long-term potentiation and for learning and memory (Molinari et al., 1996). It is markedly reduced in the dentate gyrus of many, but not all, hAPP<sub>high</sub> mice in a manner that strongly correlates with impaired performance in the Morris water maze (Palop et al., 2003). Calbindin levels in granule cells of the dentate gyrus were only slightly reduced in singly TG hAPP<sub>low</sub> mice and unaffected in singly TG FYN mice compared with NTG controls (Fig. 1). In contrast, doubly TG FYN/hAPP<sub>low</sub> mice had profound depletions of calbindin (Fig. 1*A,B*) that were similar in magnitude to those in age-matched singly TG hAPP<sub>high</sub> mice without the FYN transgene (Fig. 1*C*). These results were confirmed by Western blot analysis of dentate gyrus lysates, which demonstrated lower calbindin levels in FYN/hAPP<sub>low</sub> mice than in NTG mice and singly TG controls (Fig. 1*D*, bottom). hAPP (Fig. 1*D*, top) and Fyn levels (Fig. 1*D*, middle) are shown to illustrate the similar extent to which these proteins are overexpressed in FYN/hAPP<sub>low</sub> mice and in the corresponding singly TG controls.

Calbindin depletions in the dentate gyrus of hAPP<sub>high</sub> mice correlate tightly with reductions in Fos-positive granule cells (Palop et al., 2003). hAPP<sub>low</sub> and FYN singly TG mice had fewer Fos-positive granule cells than NTG controls (Fig. 2*A,C*), although only FYN/hAPP<sub>low</sub> mice had Fos reductions as severe as those in hAPP<sub>high</sub> mice (Fig. 2*D*). Decreases in Fos-positive granule cells correlated with calbindin reductions in mice of all TG genotypes in which Fos levels were reduced (Fig. 2*B*), suggesting that Fos and calbindin were affected by a common mechanism.

#### Fyn and hAPP/A $\beta$ decrease the activity of ERK1/2 in the dentate gyrus

The expression of Fos and other immediate-early genes is controlled by transcription factors, the nuclear translocation and transcriptional activity of which are regulated by synaptic activity-dependent kinases such as ERK1/2 (Kelleher et al., 2004; Sweatt, 2004). To test whether the reduction in Fos might be related to impaired ERK1/2 activity, we examined the expression of dually phosphorylated (activated) ERK1/2 in granule cells. Similar to the results obtained for Fos, the number of phospho-ERK1/2-positive granule cells was significantly reduced in singly TG hAPP<sub>low</sub> mice and most severely affected in FYN/hAPP<sub>low</sub> mice (Fig. 3*A–C*). Once again, the reductions in phospho-ERK1/2-positive granule cells in FYN/hAPP<sub>low</sub> mice matched those in hAPP<sub>high</sub> mice (Fig. 3*D*). The numbers of Fos-positive and phospho-ERK-positive granule cells were correlated in all groups of TG mice, suggesting that these proteins are coregulated (Fig. 3*B*).

#### Combined expression of Fyn and hAPP/A $\beta$ impairs induction of Arc expression after exploration of a novel environment

ERK1/2 also regulates the expression of the immediate-early gene product Arc (Waltereit et al., 2001; Kremerskothen et al., 2002; Ying et al., 2002). Arc is highly enriched in dendrites of hippocampal neurons where it binds to cytoskeletal elements (Lyford et al., 1995) and has been characterized for the accumulation of its mRNA and protein in segments of dendrites that were recently active (Steward et al., 1998). Exploration of a novel envi-

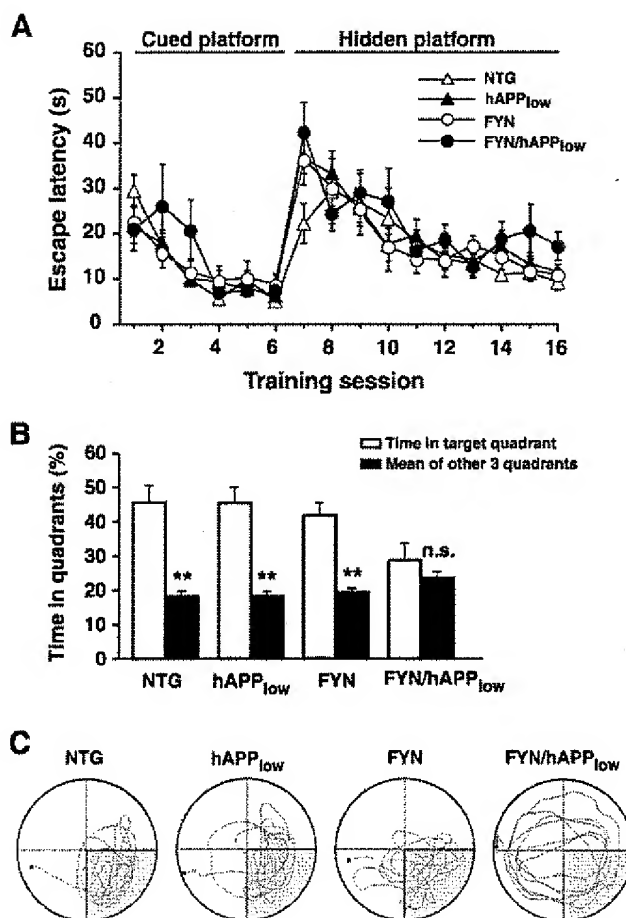


**Figure 5.** Impaired spatial memory retention in FYN/hAPP<sub>low</sub> mice. *A*, Acquisition of the cued and hidden platform portions of the Morris water maze test was similar in all groups of mice ( $n = 7$ – $11$  per genotype). *B*, During the probe trial (platform removed), FYN/hAPP<sub>low</sub> mice showed no preference for the target quadrant, whereas NTG, hAPP<sub>low</sub>, and FYN mice spent significantly more time searching the target quadrant than the other three quadrants.  $^{**}p < 0.01$  versus target quadrant by Student's  $t$  test. *C*, Representative examples of swim paths during the probe trial. Shading indicates the target quadrant.

ronment has been shown to induce Arc expression in dentate granule cells (Guzowski et al., 1999; Pinaud et al., 2001; Chawla et al., 2005). Novel environment exploration strongly increases Arc expression in granule cells of the dentate gyrus in NTG mice but not in hAPP<sub>high</sub> mice (Palop et al., 2005). In contrast, singly TG hAPP<sub>low</sub> and FYN mice showed normal Arc induction in this paradigm, although their basal Arc levels were lower than those of NTG littermates (Fig. 4*A,D*). Notably, FYN/hAPP<sub>low</sub> mice had more prominent reductions in basal Arc levels and actually showed a decrease in Arc expression instead of an increase after environmental exploration (Fig. 4*A,B,D*). No significant differences were found in locomotion or object interactions among the four genotypes (data not shown). All groups of mice showed similar basal levels of Arc and comparable Arc induction in the pyramidal cell layer of CA1 (Fig. 4*A,E*) and in the neocortex (Fig. 4*C,F*), although the induction was slightly attenuated in hAPP<sub>low</sub> and FYN/hAPP<sub>low</sub> mice. The selective deficit in basal and induced Arc expression in the dentate gyrus of doubly TG FYN/hAPP<sub>low</sub> mice is very similar to that observed in singly TG hAPP<sub>high</sub> mice (Palop et al., 2005), suggesting that Fyn and hAPP/A $\beta$  act synergistically to impair Arc expression in a brain region-specific manner.

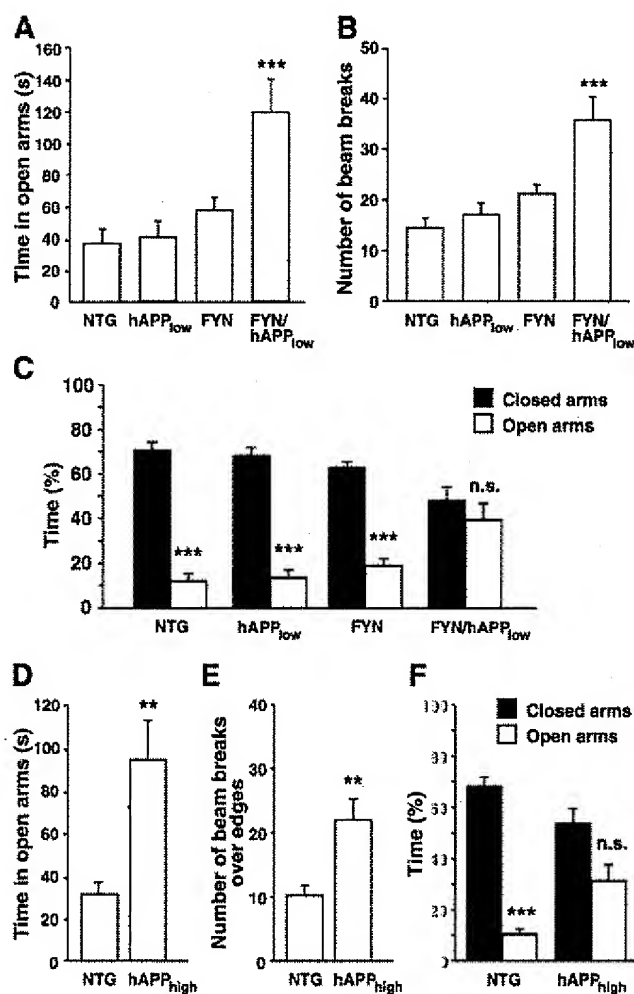


**Figure 6.** Behavioral alterations of FYN/hAPP<sub>low</sub> mice in the elevated plus maze. *A, B*, FYN/hAPP<sub>low</sub> mice spent significantly more time in the open arms (*A*) and peered more often over the edges of the maze (*B*) than the other three groups ( $n = 15$ – $25$  mice per genotype). *C*, FYN/hAPP<sub>low</sub> mice showed no preference for the closed arms, whereas NTG, hAPP<sub>low</sub>, and FYN mice spent significantly more time in the closed arms than in the open arms of the maze. *D–F*, Compared with NTG controls, singly TG hAPP<sub>high</sub> mice also spent more time in the open arms (*D*), peered over the edges of the apparatus more often (*E*), and showed no significant preference for the closed arms (*F*) ( $n = 12$ – $13$  mice per genotype).  $^{**}p < 0.01$  versus NTG by Student's *t* test (*D, E*);  $^{***}p < 0.001$  versus NTG by ANOVA (*A, B*) or versus closed arms by Student's *t* test (*C, F*).

#### Cooperation of Fyn and hAPP/A $\beta$ impairs spatial memory retention and alters emotional behavior

Because the molecules that were reduced in the dentate gyrus of FYN/hAPP<sub>low</sub> mice are critically involved in the formation or consolidation of memories (Molinari et al., 1996; Atkins et al., 1998; Blum et al., 1999; Guzowski et al., 2000; Guzowski, 2002; He et al., 2002), we next assessed the spatial learning and memory of mice in the Morris water maze. NTG, hAPP<sub>low</sub>, FYN, and FYN/hAPP<sub>low</sub> mice were able to learn both the cued (platform location visible) and the spatial (platform hidden) components of this task (Fig. 5*A*). However, when retention of spatial memory was tested in a probe trial 24 h after the last training trial, only FYN/hAPP<sub>low</sub> mice were impaired, showing no preference for the target quadrant based on comparisons of the time they spent in each quadrant (Fig. 5*B*) and of their swim paths (Fig. 5*C*). hAPP<sub>high</sub> mice have similar probe trial deficits, although many of these mice also show deficits in task acquisition (Palop et al., 2003).

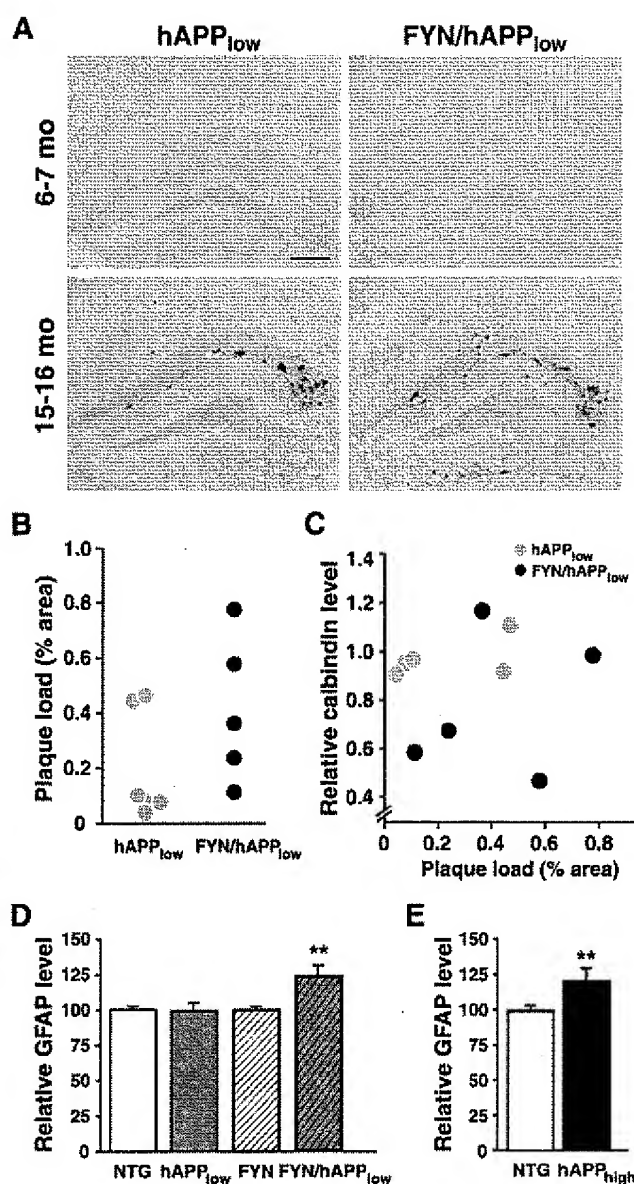


**Figure 7.** Overexpression of Fyn does not affect amyloid deposition but elicits an astroglial injury response in FYN/hAPP<sub>low</sub> mice. *A*, At 6–7 months (mo) of age (top), immunostaining for A $\beta$  revealed no amyloid deposits in hAPP<sub>low</sub> and FYN/hAPP<sub>low</sub> mice. At 15–16 months (bottom), these mice had comparable levels of amyloid deposition. *B*, Quantitation of amyloid deposition in 15- to 16-month-old mice. *C*, Plaque load did not correlate with calbindin levels in 15- to 16-month-old hAPP<sub>low</sub> or FYN/hAPP<sub>low</sub> mice. *D*, Quantitation of GFAP immunoreactivity in 6- to 7-month-old mice revealed increased astroglial GFAP expression indicative of reactive astrogliosis in FYN/hAPP<sub>low</sub> mice relative to NTG or singly TG mice ( $n = 8$ – $12$  per genotype). *E*, Age-matched hAPP<sub>high</sub> mice had similar increases in GFAP expression ( $n = 10$  per genotype).  $^{**}p < 0.01$  versus NTG by ANOVA (*D*) or Student's *t* test (*E*). Scale bar, 250  $\mu$ m.

To determine whether Fyn and hAPP/A $\beta$  may interact also in brain regions other than the dentate gyrus, we examined the behavior of the mice in the elevated plus maze, a paradigm that provides putative measures of emotionality and exploratory behaviors that are mostly independent of the hippocampus (Dawson and Tricklebank, 1995; Wall and Messier, 2001). The coexpression of FYN and hAPP<sub>low</sub> also affected the performance of mice in the elevated plus maze. FYN/hAPP<sub>low</sub> mice spent significantly more time in the open arms of the maze and poked their noses over the edges of the open arms more often than hAPP<sub>low</sub> mice, FYN mice, and NTG controls (Fig. 6*A, B*). FYN/

hAPP<sub>low</sub> mice showed no significant preference for the closed arms over the open arms of the maze, in contrast to the other three groups of mice (Fig. 6C). These behavioral alterations of FYN/hAPP<sub>low</sub> mice are remarkably similar to those of hAPP<sub>high</sub> mice in this test (Fig. 6D–F).

#### Increased Fyn expression does not affect amyloid deposition

We previously used ELISA to demonstrate that neither increasing nor ablating Fyn expression affects hippocampal A $\beta$  levels in 6- to 7-month-old mice (Chin et al., 2004). To determine whether the exacerbation of hAPP/A $\beta$ -induced neuronal and behavioral alterations by Fyn could stem from changes in the deposition of A $\beta$ , we compared A $\beta$  deposits (plaque load) in hAPP<sub>low</sub> and FYN/hAPP<sub>low</sub> mice. At 6–8 months, the age at which all other biochemical, immunohistochemical, and behavioral experiments were performed, no plaques were detected in the hippocampus of these mice (Fig. 7A, top). By 15–16 months of age, hAPP<sub>low</sub> and FYN/hAPP<sub>low</sub> mice had comparable hippocampal plaque loads (Fig. 7A, B) ( $p = 0.13$ ; Mann–Whitney  $U$  test). No correlation was found between plaque load and calbindin levels in either hAPP<sub>low</sub> or FYN/hAPP<sub>low</sub> mice (Fig. 7C) at this age.

#### Increased astroglial injury response in FYN/hAPP<sub>low</sub> mice

Astrocytes upmodulate the expression of GFAP in response to a variety of neural injuries (Eddleston and Mucke, 1993; Eng et al., 2000). We analyzed this sensitive indicator of neuronal distress at 6–8 months of age. Hippocampal GFAP levels in hAPP<sub>low</sub> and FYN mice were similar to those of NTG controls, whereas FYN/hAPP<sub>low</sub> mice had significantly higher levels of GFAP labeling (Fig. 7D). This increase in GFAP expression in FYN/hAPP<sub>low</sub> mice without plaques was similar in magnitude to that in age-matched hAPP<sub>high</sub> mice with plaques (Fig. 7E).

#### Regulation of Fyn activity in hAPP<sub>high</sub> and FYN/hAPP<sub>low</sub> mice

To determine whether hAPP/A $\beta$  actually increases Fyn activity *in vivo*, we immunoprecipitated Fyn from dentate gyrus lysates of hAPP<sub>high</sub> mice and examined the levels of Tyr<sup>416</sup> phosphorylation with a phospho-specific antibody. Phosphorylation at this site activates Fyn and is indicative of kinase activity (Nguyen et al., 2002; Roskoski, 2004; Santucci et al., 2005). In hAPP<sub>high</sub> mice with relatively preserved levels of calbindin (higher than the average of all hAPP<sub>high</sub> mice), levels of active Fyn were similar to those in NTG mice. In contrast, hAPP<sub>high</sub> mice with prominent depletions of calbindin (levels lower than the average of all hAPP<sub>high</sub> mice) exhibited decreased levels of active Fyn (Fig. 8A). Notably, our previous studies demonstrated that the extent of calbindin depletion in hAPP<sub>high</sub> mice correlates tightly with the severity of learning and memory deficits in the Morris water maze test (Palop et al., 2003).

Next, we examined whether levels of active Fyn were also different in FYN and FYN/hAPP<sub>low</sub> mice. Although levels of total Fyn were similar in these groups (Figs. 1D, 8B, bottom blot), levels of active Fyn were strikingly lower in FYN/hAPP<sub>low</sub> mice than in FYN mice (Fig. 8B).

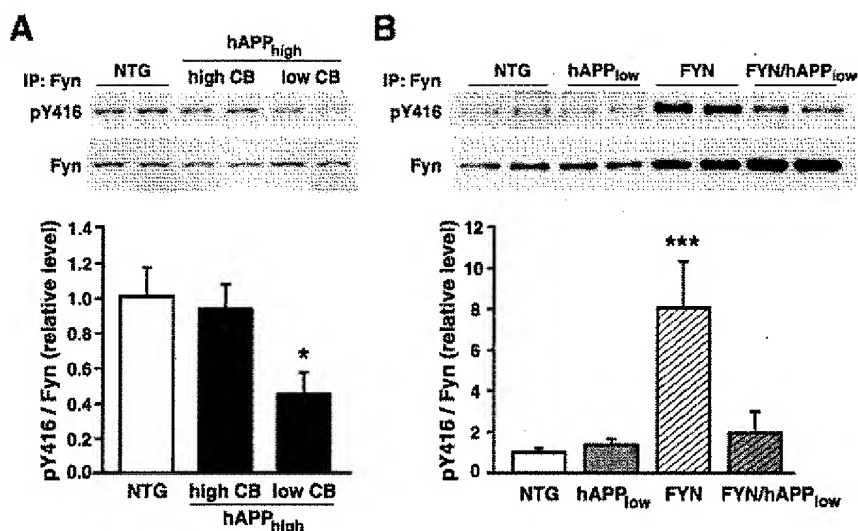


**Figure 8.** Decreased levels of active Fyn in the dentate gyrus of hAPP<sub>high</sub> and FYN/hAPP<sub>low</sub> mice. Total Fyn was immunoprecipitated from isolated dentate gyri of 2- to 3-month-old mice and analyzed by Western blot using antibodies that recognize active Fyn (pY416) or both active and inactive Fyn. **A**, Levels of active Fyn were decreased in hAPP<sub>high</sub> mice with depletions of calbindin in the dentate gyrus but not in hAPP<sub>high</sub> mice with relatively normal levels of calbindin ( $n = 4$ –9 per group). **B**, Singly TG FYN mice exhibited expected increases in active Fyn, but this increase was attenuated in FYN/hAPP<sub>low</sub> mice ( $n = 3$ –5 per genotype). \* $p < 0.05$ , \*\*\* $p < 0.001$  versus NTG by ANOVA.

#### Concurrent increases in STEP and $\alpha 7$ nAChR in hAPP<sub>high</sub> and FYN/hAPP<sub>low</sub> mice

What regulatory mechanisms might underlie the surprising downmodulation of Fyn in hAPP<sub>high</sub> and FYN/hAPP<sub>low</sub> mice? To begin to address this question, we measured the 61 kDa form of STEP, which associates with and dephosphorylates Fyn at the regulatory Tyr<sup>416</sup> (Nguyen et al., 2002). STEP is present at postsynaptic densities of glutamatergic synapses and interacts with both src kinase family members and NMDA receptors, opposing src-mediated upregulation of NMDA receptors (Pelkey et al., 2002). STEP levels were indeed significantly increased in the dentate gyrus of hAPP<sub>high</sub> mice relative to NTG controls (Fig. 9A). Because A $\beta$  has recently been shown to activate STEP in cultured neurons via  $\alpha 7$  nAChRs (Snyder et al., 2005), we measured  $\alpha 7$  nAChR levels in the dentate gyrus of our mice. The  $\alpha 7$  nAChR levels were approximately twice as high in hAPP<sub>high</sub> mice as in NTG controls (Fig. 9B), indicating that A $\beta$  engages this pathway also *in vivo*.

Finally, we examined whether STEP and  $\alpha 7$  nAChRs were also increased in the dentate gyrus of FYN/hAPP<sub>low</sub> mice. Compared with NTG and FYN mice, FYN/hAPP<sub>low</sub> mice had approximately twofold higher levels of STEP and fivefold higher levels of  $\alpha 7$  nAChRs (Fig. 9C–E). STEP levels were also increased in singly TG hAPP<sub>low</sub> mice, although to lesser extent than in FYN/hAPP<sub>low</sub> mice (Fig. 9C,D).

#### Discussion

The current study demonstrates that increased neuronal expression of Fyn can promote hAPP/A $\beta$ -dependent neuronal and behavioral deficits that may be relevant to the cognitive decline in AD. Elevating neuronal expression of Fyn in hAPP<sub>low</sub> mice with relatively minor neuronal deficits created a striking phenocopy of the more severe deficits seen in hAPP<sub>high</sub> mice.

In considering the different possibilities in which Fyn and A $\beta$  might interact, it is not unreasonable to speculate that Fyn actually mediates the detrimental effects of A $\beta$ . However, our measurements of Fyn activity suggest that Fyn could also act as a

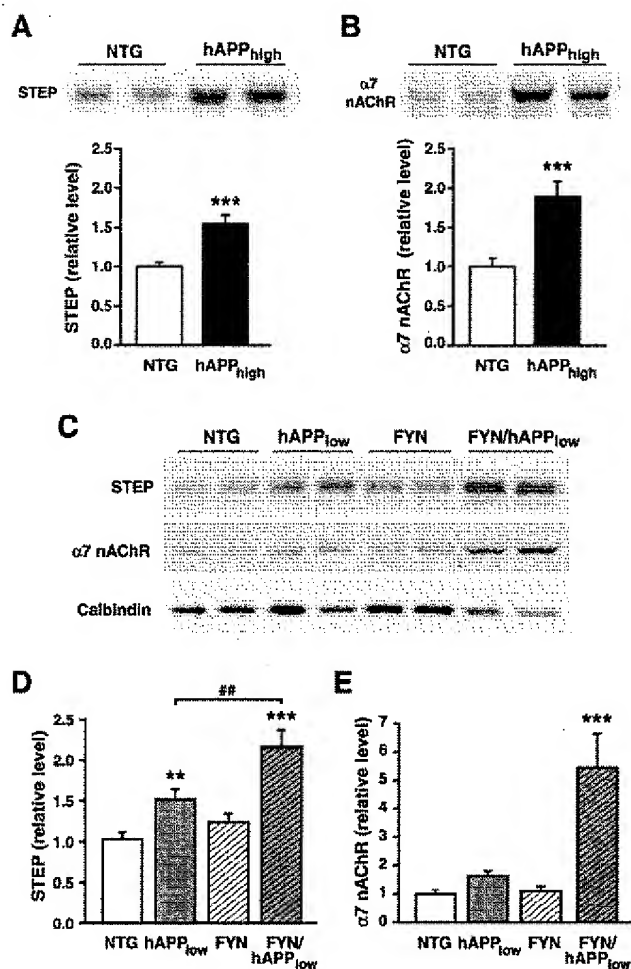


**Figure 9.** STEP and  $\alpha 7$  nAChRs are elevated in the dentate gyrus of hAPP<sub>high</sub> and FYN/hAPP<sub>low</sub> mice. *A*, Levels of the 61 kDa form of STEP in the dentate gyrus were higher in hAPP<sub>high</sub> mice than in NTG controls ( $n = 11$ –12 per genotype). *B*, Levels of  $\alpha 7$  nAChRs in the dentate gyrus were also significantly elevated in hAPP<sub>high</sub> mice ( $n = 7$  per genotype). *C*, Representative Western blots illustrating STEP,  $\alpha 7$  nAChR, and calbindin levels in the dentate gyrus of NTG, hAPP<sub>low</sub>, FYN, and FYN/hAPP<sub>low</sub> mice. *D*, *E*, Quantitation of STEP (*D*) and  $\alpha 7$  nAChR (*E*) levels demonstrates twofold to fivefold increases in these proteins in FYN/hAPP<sub>low</sub> mice relative to NTG controls ( $n = 8$ –12 per genotype). \*\*\* $p < 0.001$  versus NTG by Student's  $t$  test; (*A*, *B*); \*\* $p < 0.01$ , \*\*\* $p < 0.001$  versus NTG by ANOVA; \*\* $p < 0.01$  by PLSD *post hoc* test (*D*).

separate copathogenic factor that converges onto similar or identical downstream targets. Compared with NTG controls, hAPP<sub>high</sub> and FYN/hAPP<sub>low</sub> mice had more severe neuronal and behavioral deficits than hAPP<sub>low</sub> and FYN mice. Yet, Fyn activity was lower in hAPP<sub>high</sub> mice than in NTG controls and was also lower in FYN/hAPP<sub>low</sub> mice than in FYN mice. These findings suggest the involvement of complex regulatory mechanisms that may become engaged to protect neurons against synergistic effects of A $\beta$  and Fyn.

In line with this interpretation, we found significant increases in levels of STEP, a phosphatase that inactivates Fyn, in both hAPP<sub>high</sub> and FYN/hAPP<sub>low</sub> mice. STEP opposes the phosphorylation of src family kinase substrates such as Tyr<sup>1472</sup> of the NR2B subunit of NMDARs (Pelkey et al., 2002). Interestingly, hAPP<sub>high</sub> mice have significant decreases in levels of phospho-Tyr<sup>1472</sup> of NR2B (Palop et al., 2005), consistent with the increased STEP levels and suppressed Fyn activity we detected in these mice in the current study. A $\beta$ -induced activation of STEP also led to reduced phospho-Tyr<sup>1472</sup> of NR2B in cultured neurons, resulting in en-

docytoysis of the receptor and reduced NMDAR-mediated signaling (Snyder et al., 2005). The study by Snyder et al. (2005) also demonstrated that A $\beta$  can recruit STEP via  $\alpha 7$  nAChR-dependent signaling. Our identification of abnormally high  $\alpha 7$  nAChR levels in both hAPP<sub>high</sub> and FYN/hAPP<sub>low</sub> mice highlights the potential functional relevance of this pathway *in vivo*. Indeed, increased levels of nAChRs and STEP in hAPP<sub>high</sub> and FYN/hAPP<sub>low</sub> mice were associated with depletions of synaptic activity-related proteins that are known to correlate tightly with deficits in learning and memory (Palop et al., 2003, 2005). Unlike the majority of membrane-bound receptors, nAChR expression is increased after receptor stimulation (Fenster et al., 1999), supporting the notion of increased signaling through  $\alpha 7$  nAChRs in hAPP<sub>high</sub> and FYN/hAPP<sub>low</sub> mice. A $\beta$  and Fyn activities may also converge on other cell-surface molecules, including integrins and NMDARs, and these possibilities deserve to be tested in future studies.

Independent of the precise relationship between A $\beta$  and Fyn-related signaling pathways, the results presented here clearly demonstrate that increased neuronal Fyn expression can critically exacerbate neuronal and behavioral impairments in the context of even relatively moderate increases in A $\beta$  production. The similarity of impairments in FYN/hAPP<sub>low</sub> and hAPP<sub>high</sub> mice was essentially complete with respect to molecular alterations and somewhat less complete with respect to behavioral deficits. In the water maze test, FYN/hAPP<sub>low</sub> mice were impaired only in retention of spatial memory assessed by the 24 h probe trial, which provides a sensitive measure of hippocampus-dependent function (Lipp and Wolfer, 1998; Wolfer et al., 1998). In contrast, hAPP<sub>high</sub> mice were also impaired in task acquisition (Palop et al., 2003). Thus, Fyn signaling may play a more prominent role in hippocampus-dependent memory retention deficits than in acquisition deficits. The possibility of such dissociations is highlighted by our previous study (Chin et al., 2004), which demonstrated that hAPP/A $\beta$ -dependent premature mortality and loss of synaptophysin are modulated by Fyn, whereas aberrant axonal sprouting is not.

Although singly TG FYN and hAPP<sub>low</sub> mice had no behavioral alterations, both groups showed some depletion of synaptic activity-dependent proteins in granule cells of the dentate gyrus. Although these depletions were less severe than those in hAPP<sub>high</sub> and FYN/hAPP<sub>low</sub> mice, they demonstrate that increased neuronal expression of Fyn is sufficient to elicit molecular alterations similar to those induced by moderate levels of hAPP/A $\beta$ . These findings also suggest that our molecular outcome measures may be more sensitive than the behavioral tests we used in this study.

Because reductions in Fos, Arc, and ERK1/2 can contribute to deficits in learning and memory (Molinari et al., 1996; Atkins et al., 1998; Blum et al., 1999; Guzowski, 2002; He et al., 2002), it is possible that the neuronal network can compensate for the relatively subtle reduction of these factors in FYN and hAPP<sub>low</sub> mice but is overcome by their more severe depletion in hAPP<sub>high</sub> and FYN/hAPP<sub>low</sub> mice, resulting in behavioral decompensation. Consistent with this hypothesis, Arc induction was normal in FYN mice and in hAPP<sub>low</sub> mice, suggesting that activity-regulated gene expression was normal. However, there was no induction of Arc in FYN/hAPP<sub>low</sub> mice that explored a novel environment. In fact, these mice had even fewer Arc-positive granule cells than home-caged FYN/hAPP<sub>low</sub> mice, suggesting a paradoxical response of these cells or of the network to which they belong.

FYN/hAPP<sub>low</sub> mice also exhibited altered behavior in the elevated plus maze in a manner similar to hAPP<sub>high</sub> mice. This test is



used to measure emotional behaviors that are mostly independent of the hippocampus (Dawson and Tricklebank, 1995; Wall and Messier, 2001). Thus, the alterations observed in FYN/hAPP<sub>low</sub> mice in this test suggest that activities of Fyn and hAPP/A $\beta$  may interact also in brain regions other than the dentate gyrus. In addition, they suggest that this interaction can contribute not only to memory deficits, but also to alterations in emotional behavior, which afflict both hAPP mice and AD patients (Terry et al., 1991; Cummings and Kaufer, 1996; Lee et al., 2004).

Although increased production of A $\beta$  may be sufficient to cause early-onset autosomal-dominant AD (Tanzi and Bertram, 2005), the much more frequent cases of late-onset "sporadic" AD are likely caused by the combination of different genetic and environmental risk factors (Mayeux, 2003; Kamboh, 2004; Tanzi and Bertram, 2005). It will be interesting to determine whether some of these risk factors elevate Fyn activity, because our findings suggest that this process could synergize with A $\beta$  to induce neuronal dysfunction. Indeed, increases in neuronal Fyn expression triggered hAPP/A $\beta$ -dependent behavioral deficits and worsened the depletion of multiple factors involved in synaptic plasticity.

It is noteworthy in this context that 6- to 8-month-old FYN/hAPP<sub>low</sub> mice had not yet formed amyloid plaques but in most molecular and behavioral measures were as severely impaired as plaque-bearing hAPP<sub>high</sub> mice of the same age. This finding extends to the molecular level the hypothesis that A $\beta$ -induced behavioral deficits in hAPP mice are primarily plaque independent (Holcomb et al., 1999; Hsia et al., 1999; Westerman et al., 2002; Palop et al., 2003). Indeed, our results are most consistent with the hypothesis that Fyn promotes the pathogenic effects of small nonfibrillar A $\beta$  assemblies (Lambert et al., 1998), although interactions with alternative hAPP metabolites have not yet been excluded. Studies are needed to determine whether therapeutic manipulations of Fyn or related pathways could protect the aging brain against pathogenic A $\beta$  assemblies and AD-related neurological decline.

## References

- Arancio O, Zhang HP, Chen X, Lin C, Trinchese F, Puzzo D, Liu S, Hegde A, Yan SF, Stern A, Luddy JS, Lue LF, Walker DG, Roher A, Buttini M, Mucke L, Li W, Schmidt AM, Kindy M, Hyslop PA, et al. (2004) RAGE potentiates A $\beta$ -induced perturbation of neuronal function in transgenic mice. *EMBO J* 23:4096–4105.
- Atkins CM, Selcher JC, Petraitis JJ, Trzaskos JM, Sweatt JD (1998) The MAPK cascade is required for mammalian associative learning. *Nat Neurosci* 1:602–609.
- Bi X, Gall CM, Zhou J, Lynch G (2002) Uptake and pathogenic effects of amyloid beta peptide 1–42 are enhanced by integrin antagonists and blocked by NMDA receptor antagonists. *Neuroscience* 112:827–840.
- Blum S, Moore AN, Adams F, Dash PK (1999) A mitogen-activated protein kinase cascade in the CA1/CA2 subfield of the dorsal hippocampus is essential for long-term spatial memory. *J Neurosci* 19:3535–3544.
- Chawla MK, Guzowski JF, Ramirez-Amaya V, Lipa P, Hoffman KL, Marriott LK, Worley PF, McNaughton BL, Barnes CA (2005) Sparse, environmentally selective expression of Arc RNA in the upper blade of the rodent fascia dentata by brief spatial experience. *Hippocampus* 15:579–586.
- Chin J, Palop JJ, Yu G-Q, Kojima N, Masliah E, Mucke L (2004) Fyn kinase modulates synaptotoxicity, but not aberrant sprouting, in human amyloid precursor protein transgenic mice. *J Neurosci* 24:4692–4697.
- Cummings JL, Kaufer D (1996) Neuropsychiatric aspects of Alzheimer's disease: the cholinergic hypothesis revisited. *Neurology* 47:876–883.
- Dawson GR, Tricklebank MD (1995) Use of the elevated plus maze in the search for novel anxiolytic agents. *Trends Pharmacol Sci* 16:33–36.
- Dineley KT, Westerman M, Bui D, Bell K, Ashe KH, Sweatt JD (2001)  $\beta$ -Amyloid activates the mitogen-activated protein kinase cascade via hippocampal  $\alpha 7$  nicotinic acetylcholine receptors: *in vitro* and *in vivo* mechanisms related to Alzheimer's disease. *J Neurosci* 21:4125–4133.
- Eddleston MP, Mucke L (1993) Molecular profile of reactive astrocytes—implications for their role in neurologic disease. *Neuroscience* 54:15–36.
- Eng LF, Ghirnikar RS, Lee YL (2000) Glial fibrillary acidic protein: GFAP—thirty-one years (1969–2000). *Neurochem Res* 25:1439–1451.
- Fenster CP, Whitworth TL, Sheffield EB, Quick MW, Lester RA (1999) Up-regulation of surface  $\alpha 4\beta 2$  nicotinic receptors is initiated by receptor desensitization after chronic exposure to nicotine. *J Neurosci* 19:4804–4814.
- Gotz J, Streffer J, David D, Schild A, Hoernndli F, Pennanen L, Kurosinski P, Chen F (2004) Transgenic animal models of Alzheimer's disease and related disorders: histopathology, behavior and therapy. *Mol Psychiatry* 9:664–683.
- Grace EA, Rabiner CA, Busciglio J (2002) Characterization of neuronal dystrophy induced by fibrillar amyloid  $\beta$ : implications for Alzheimer's disease. *Neuroscience* 114:265–273.
- Guzowski JF (2002) Insights into immediate-early gene function in hippocampal memory consolidation using antisense oligonucleotide and fluorescent imaging approaches. *Hippocampus* 12:86–104.
- Guzowski JF, McNaughton BL, Barnes CA, Worley PF (1999) Environment-specific expression of the immediate-early gene Arc in hippocampal neuronal ensembles. *Nat Neurosci* 2:1120–1124.
- Guzowski JF, Lyford GL, Stevenson GD, Houston FP, McGaugh JL, Worley PF, Barnes CA (2000) Inhibition of activity-dependent arc protein expression in the rat hippocampus impairs the maintenance of long-term potentiation and the consolidation of long-term memory. *J Neurosci* 20:3993–4001.
- He J, Yamada K, Nabeshima T (2002) A role of Fos expression in the CA3 region of the hippocampus in spatial memory formation in rats. *Neuropsychopharmacology* 26:259–268.
- Higgins GA, Jacobsen H (2003) Transgenic mouse models of Alzheimer's disease: phenotype and application. *Behav Pharmacol* 14:419–438.
- Ho G, Drego R, Hakimian E, Hashimoto M, Tong G, Thai L, Masliah E (2004) Involvement of Fyn and MAP kinase signaling in synaptic loss in Alzheimer's disease. *Soc Neurosci Abstr* 30:218.5.
- Holcomb LA, Gordon MN, Jantzen P, Hsiao K, Duff K, Morgan D (1999) Behavioral changes in transgenic mice expressing both amyloid precursor protein and presenilin-1 mutations: lack of association with amyloid deposits. *Behav Genet* 29:177–185.
- Hsia A, Masliah E, McConlogue L, Yu G, Tatsuno G, Hu K, Kholodenko D, Malenka RC, Nicoll RA, Mucke L (1999) Plaque-independent disruption of neural circuits in Alzheimer's disease mouse models. *Proc Natl Acad Sci USA* 96:3228–3233.
- Kamboh MI (2004) Molecular genetics of late-onset Alzheimer's disease. *Ann Hum Genet* 68:381–404.
- Kelleher III RJ, Govindarajan A, Tonegawa S (2004) Translational regulatory mechanisms in persistent forms of synaptic plasticity. *Neuron* 44:59–73.
- Kennedy MB (1997) The postsynaptic density at glutamatergic synapses. *Trends Neurosci* 20:264–268.
- Klein WL, Krafft GA, Finch CE (2001) Targeting small A $\beta$  oligomers: the solution to an Alzheimer's disease conundrum. *Trends Neurosci* 24:219–224.
- Kobayashi DT, Chen KS (2005) Behavioral phenotypes of amyloid-based genetically modified mouse models of Alzheimer's disease. *Genes Brain Behav* 4:173–196.
- Kojima N, Wang J, Mansuy IM, Grant SGN, Mayford M, Kandel ER (1997) Rescuing impairment of long-term potentiation in fyn-deficient mice by introducing Fyn transgene. *Proc Natl Acad Sci USA* 94:4761–4765.
- Kojima N, Ishibashi H, Obata K, Kandel ER (1998) Higher seizure susceptibility and enhanced tyrosine phosphorylation on N-methyl-D-aspartate receptor subunit 2B in fyn transgenic mice. *Learn Mem* 5:429–445.
- Kremerskothen J, Wendholt D, Teber I, Barnekow A (2002) Insulin-induced expression of the activity-regulated cytoskeleton-associated gene (ARC) in human neuroblastoma cells requires p21(ras), mitogen-activated protein kinase/extracellular regulated kinase and src tyrosine kinases but is protein kinase C-independent. *Neurosci Lett* 321:153–156.
- Lambert MP, Barlow AK, Chromy BA, Edwards C, Freed R, Liosatos M, Morgan TE, Rozovsky I, Trommer B, Viola KL, Wals P, Zhang C, Finch CE, Krafft GA, Klein WL (1998) Diffusible, nonfibrillar ligands derived

- from A $\beta_{1-42}$  are potent central nervous system neurotoxins. *Proc Natl Acad Sci USA* 95:6448–6453.
- Lee KW, Lee SH, Kim H, Song JS, Yang SD, Paik SG, Han PL (2004) Progressive cognitive impairment and anxiety induction in the absence of plaque deposition in C57BL/6 inbred mice expressing transgenic amyloid precursor protein. *J Neurosci Res* 76:572–580.
- Lipp HP, Wolfer DP (1998) Genetically modified mice and cognition. *Curr Opin Neurobiol* 8:272–280.
- Lyford GL, Yamagata K, Kaufmann WE, Barnes CA, Sanders LK, Copeland NG, Gilbert DJ, Jenkins NA, Lanahan AA, Worley PF (1995) *Arc*, a growth factor and activity-regulated gene, encodes a novel cytoskeleton-associated protein that is enriched in neuronal dendrites. *Neuron* 14:433–445.
- Mayeux R (2003) Epidemiology of neurodegeneration. *Annu Rev Neurosci* 26:81–104.
- Molinari S, Battini R, Ferrari S, Pozzi L, Killcross AS, Robbins TW, Jouvenceau A, Billard J-M, Dutar P, Lamour Y, Baker WA, Cox H, Emson PC (1996) Deficits in memory and hippocampal long-term potentiation in mice with reduced calbindin D<sub>28k</sub> expression. *Proc Natl Acad Sci USA* 93:8028–8033.
- Mucke L, Abraham CR, Ruppe MD, Rockenstein EM, Toggas SM, Alford M, Masliah E (1995) Protection against HIV-1 gp120-induced brain damage by neuronal expression of human amyloid precursor protein. *J Exp Med* 181:1551–1556.
- Mucke L, Masliah E, Yu G-Q, Mallory M, Rockenstein EM, Tatsuno G, Hu K, Kholodenko D, Johnson-Wood K, McConlogue L (2000) High-level neuronal expression of A $\beta_{1-42}$  in wild-type human amyloid protein precursor transgenic mice: synaptotoxicity without plaque formation. *J Neurosci* 20:4050–4058.
- Nguyen TH, Liu J, Lombroso PJ (2002) Striatal enriched phosphatase 61 dephosphorylates. Fyn at phosphotyrosine 420. *J Biol Chem* 277:24274–24279.
- Palop JJ, Jones B, Kekoni L, Chin J, Yu G-Q, Raber J, Masliah E, Mucke L (2003) Neuronal depletion of calcium-dependent proteins in the dentate gyrus is tightly linked to Alzheimer's disease-related cognitive deficits. *Proc Natl Acad Sci USA* 100:9572–9577.
- Palop JJ, Chin J, Bien-Ly N, Massaro C, Yeung BZ, Yu G-Q, Mucke L (2005) Vulnerability of dentate granule cells to disruption of *Arc* expression in human amyloid precursor protein transgenic mice. *J Neurosci* 25:9686–9693.
- Pelkey KA, Askalan R, Paul S, Kalia LV, Nguyen TH, Pitcher GM, Salter MW, Lombroso PJ (2002) Tyrosine phosphatase STEP is a tonic brake on induction of long-term potentiation. *Neuron* 34:127–138.
- Pinaud R, Penner MR, Robertson HA, Currie RW (2001) Upregulation of the immediate early gene *arc* in the brains of rats exposed to environmental enrichment: Implications for molecular plasticity. *Mol Brain Res* 91:50–56.
- Raber J, Akana SF, Bhatnagar S, Dallman MF, Wong D, Mucke L (2000) Hypothalamic-pituitary-adrenal function in *ApoE*<sup>−/−</sup> mice: possible role in behavioral and metabolic alterations. *J Neurosci* 20:2064–2071.
- Rockenstein EM, McConlogue L, Tan H, Gordon M, Power M, Masliah E, Mucke L (1995) Levels and alternative splicing of amyloid  $\beta$  protein precursor (APP) transcripts in brains of transgenic mice and humans with Alzheimer's disease. *J Biol Chem* 270:28257–28267.
- Roskoski Jr R (2004) Src protein-tyrosine kinase structure and regulation. *Biochem Biophys Res Commun* 324:1155–1164.
- Sabo S, Lambert MP, Kessey K, Wade W, Krafft G, Klein WL (1995) Interaction of  $\beta$ -amyloid peptides with integrins in a human nerve cell line. *Neurosci Lett* 184:25–28.
- Salter MW, Kalia LV (2004) Src kinases: a hub for NMDA receptor regulation. *Nat Rev Neurosci* 5:317–328.
- Santucci A, Sytnyk V, Leshchynska I, Schachner M (2005) Prion protein recruits its neuronal receptor NCAM to lipid rafts to activate p59<sup>fyn</sup> and to enhance neurite outgrowth. *J Cell Biol* 169:341–354.
- Shirazi SK, Wood JG (1993) The protein tyrosine kinase, fyn, in Alzheimer's disease pathology. *NeuroReport* 4:435–437.
- Snyder EM, Nong Y, Almeida CG, Paul S, Moran T, Choi EY, Nairn AC, Salter MW, Lombroso PJ, Gouras GK, Greengard P (2005) Regulation of NMDA receptor trafficking by amyloid- $\beta$ . *Nat Neurosci* 8:1051–1058.
- Steward O, Wallace CS, Lyford GL, Worley PF (1998) Synaptic activation causes the mRNA for the IEG *Arc* to localize selectively near activated postsynaptic sites on dendrites. *Neuron* 21:741–751.
- Sweatt JD (2004) Mitogen-activated protein kinases in synaptic plasticity and memory. *Curr Opin Neurobiol* 14:311–317.
- Tanzi R, Bertram L (2005) Twenty years of the Alzheimer's disease amyloid hypothesis: a genetic perspective. *Cell* 120:545–555.
- Terry RD, Masliah E, Salmon DP, Butters N, DeTeresa R, Hill R, Hansen LA, Katzman R (1991) Physical basis of cognitive alterations in Alzheimer's disease: synapse loss is the major correlate of cognitive impairment. *Ann Neurol* 30:572–580.
- Thomas SM, Brugge JS (1997) Cellular functions regulated by src family kinases. *Cell Dev Biol* 13:513–609.
- Toggas SM, Masliah E, Rockenstein EM, Rall GF, Abraham CR, Mucke L (1994) Central nervous system damage produced by expression of the HIV-1 coat protein gp120 in transgenic mice. *Nature* 367:188–193.
- Turner PR, O'Connor K, Tate WP, Abraham WC (2003) Roles of amyloid precursor protein and its fragments in regulating neural activity, plasticity and memory. *Prog Neurobiol* 70:1–32.
- Verdier Y, Penke B (2004) Binding sites of amyloid beta-peptide in cell plasma membrane and implications for Alzheimer's disease. *Curr Protein Pept Sci* 5:19–31.
- Wall PM, Messier C (2001) Methodological and conceptual issues in the use of the elevated plus-maze as a psychological measurement instrument of animal anxiety-like behavior. *Neurosci Biobehav Rev* 25:275–286.
- Walsh DM, Selkoe DJ (2004) Deciphering the molecular basis of memory failure in Alzheimer's disease. *Neuron* 44:181–193.
- Waltereit R, Dammermann B, Wulff P, Scafidi J, Staubli U, Kauselmann G, Bundman M, Kuhl D (2001) Arg3.1/*Arc* mRNA induction by Ca<sup>2+</sup> and cAMP requires protein kinase A and mitogen-activated protein kinase/extracellular regulated kinase activation. *J Neurosci* 21:5484–5493.
- Westerman MA, Cooper-Blacketer D, Mariash A, Kotilinek L, Kawarabayashi T, Younkin LH, Carlson GA, Younkin SG, Ashe KH (2002) The relationship between A $\beta$  and memory in the Tg2576 mouse model of Alzheimer's disease. *J Neurosci* 22:1858–1867.
- Williamson R, Scales T, Clark BR, Gibb G, Reynolds CH, Kellie S, Bird IN, Varndell IM, Sheppard PW, Everall I, Anderton BH (2002) Rapid tyrosine phosphorylation of neuronal proteins including tau and focal adhesion kinase in response to amyloid- $\beta$  peptide exposure: Involvement of Src family protein kinases. *J Neurosci* 22:10–20.
- Wolfer DP, Stagliar-Bozicevic M, Errington ML, Lipp HP (1998) Spatial memory and learning in transgenic mice: fact or artifact? *News Physiol Sci* 13:118–123.
- Yaar M, Zhai S, Pilch PF, Doyle SM, Eisenhauer PB, Fine RE, Gilchrist BA (1997) Binding of beta-amyloid to the p75 neurotrophin receptor induces apoptosis—a possible mechanism for Alzheimer's disease. *J Clin Invest* 100:2333–2340.
- Yan SD, Chen X, Fu J, Chen M, Zhu HJ, Roher A, Slattery T, Zhao L, Nagashima M, Morser J, Migheli A, Nawroth P, Stern D, Schmidt AM (1996) RAGE and amyloid- $\beta$  peptide neurotoxicity in Alzheimer's disease. *Nature* 382:685–691.
- Ying SW, Futter M, Rosenblum K, Webber MJ, Hunt SP, Bliss TV, Bramham CR (2002) Brain-derived neurotrophic factor induces long-term potentiation in intact adult hippocampus: requirement for ERK activation coupled to CREB and upregulation of *Arc* synthesis. *J Neurosci* 22:1532–1540.